



Design and testing of folding Solar Cell Arrays for PocketQubes

BACHELOR FINAL THESIS

Document:

Report

Author:

Gonzalo Campos Bertrán

Director/Co-director:

Miquel Sureda Anfres / David González Diez

Degree:

Bachelor in Aerospace Engineering Technologies

Examination session:

Spring 2024

Abstract

Keywords: Deployable solar cell, PocketQube satellite, HORUS project, solar wing, iterative design, COTS components

This project has as its objective to design, build and test a deployable solar cell system for a PocketQube standard satellite, as part of the research of the HORUS project inside the UPC Space Program.

Firstly, a design concept has been selected through the research of the state of the art and the feasibility of all the subsystems according to the project requirements. The deployment mechanism has been selected, resulting in a Solar Wing configuration with tape spring deployment and bolted hinges configuration. The solar cell model and power output have also been defined, opting for a double Solar Wing and 6 cells configuration. Finally, the holding mechanism has been chosen, using a Nylon thread and a burning wire method.

Then, through iterative design using SolidWorks, a working model has been designed and built, making use of 3D printed materials and COTS components. After various prototypes of increasing complexity, the model and the deployment system performances have been considered satisfactory. Next, the 3D model has been subjected to structural and modal analysis using ANSYS, and taking into account the expected conditions during launch and imposed by regulations. The results have demonstrated that the model can perfectly withstand such conditions.

Finally, the design has been subjected to a random vibration test, making sure that the structure is prepared to survive all the mission phases. The model has successfully passed the test, proving the design. Then, the 3P design has been escalated to 1P, 1.5P, 2P and 2.5P configurations, although COTS availability has been a noticeable issue in this matter, specially for smaller configurations.

In conclusion, the design model has presented an excellent performance, proving more than capable for its intended mission. The main concern has been the availability of COTS solar cells for small configurations, causing a low power to volume ratio. Although some further study should be performed, the general subsystem is functional and ready to be integrated with the rest of the satellite.

Resumen

Palabras clave: Células solares desplegables, satélite PocketQube, proyecto HORUS, ala solar, diseño iterativo, componentes comerciales

Este proyecto tiene como objetivo diseñar, construir y probar un sistema de despliegue de placas solares para un satélite de tipo PocketQube, como parte de la investigación del proyecto HORUS dentro del UPC Space Program.

En primer lugar, se ha seleccionado un concepto de diseño a través de la investigación de picosatélites similares y la viabilidad de todos los subsistemas de acuerdo con los requisitos del proyecto. Se ha seleccionado el mecanismo de despliegue, resultando en una configuración de Ala Solar que usa un despliegue con cinta métrica y bisagras. También se ha definido el modelo de célula solar y la potencia generada, optando por una configuración de doble Ala Solar y 6 células. Finalmente, se ha elegido el mecanismo de sujeción, utilizando un método de hilo de Nylon y resistencia.

Luego, a través de un diseño iterativo utilizando SolidWorks, se ha diseñado y construido un modelo funcional, haciendo uso de materiales impresos en 3D y componentes comerciales. Tras varios prototipos de creciente complejidad, el modelo y el comportamiento del sistema de despliegue se han considerado satisfactorios. A continuación, el modelo 3D ha sido sometido a análisis estructurales y modales mediante ANSYS, teniendo en cuenta las condiciones esperadas durante el lanzamiento y las impuestas por las regulaciones. Los resultados han demostrado que el modelo puede soportar perfectamente dichas condiciones.

Finalmente, el diseño ha sido sometido a una prueba de vibración aleatoria, asegurando que la estructura está preparada para sobrevivir a todas las fases de la misión. El modelo ha pasado exitosamente la prueba, demostrando la funcionalidad diseño. Luego, el diseño en 3P se ha escalado a configuraciones de 1P, 1.5P, 2P y 2.5P, aunque la disponibilidad de componentes comerciales ha sido un problema a considerar en este aspecto, especialmente para las configuraciones más pequeñas.

En conclusión, el diseño ha presentado un rendimiento excelente, demostrando ser más que capaz para su misión prevista. La principal preocupación ha sido la disponibilidad de células solares comerciales para configuraciones pequeñas, causando una baja relación de potencia a volumen. Aunque se podría realizar algún estudio adicional, el subsistema general es funcional y está listo para ser integrado con el resto del satélite.

Contents

1	Introduction	1
1.1	Object	1
1.2	Scope	1
1.3	Requirements	2
1.4	Rationale	2
2	Review of the state of the art	4
2.1	The PocketQube standard	4
2.2	Deployable solar panels in PQ	5
2.2.1	FOSSA Systems	7
2.2.2	Alba Orbital	7
2.2.3	Other companies	8
2.2.4	Research projects	8
3	Methodology	9
3.1	Folding mechanism selection	9
3.2	Solar cell selection	11
3.3	Power estimation	12
3.4	Hinge mechanism selection	14
3.5	Hold Down Release Mechanism selection	16
3.6	Structural design	18
3.6.1	Prototype 1	18
3.6.2	Prototype 2	21
3.6.3	Prototype 3	23
3.6.4	Final design	25
3.7	Electrical design	30
3.7.1	Components selection	30
3.7.2	Circuit design	32
3.8	Simulation analysis	33
3.8.1	Model preparation and meshing	33

3.8.2 Structural analysis	35
3.8.3 Modal analysis	39
3.9 Testing	45
3.10 Scalability to other configurations	50
4 Budget summary	52
5 Analysis and assessment of environmental and social implications	53
6 Conclusions	55
6.1 Further development	55

List of Figures

1.1	Nanosatellite launches by types (Source: [1])	3
2.1	PocketQube launches with deployable solar panels since 2013 (Source: Own elaboration)	5
2.2	Components Envelope and Allowable Additional Envelope for Deployables (Source: [5])	6
2.3	FossaSat-1 (left) and a FossaSat 2E (right) (Source: [11])	7
2.4	Unicorn-1 (left) and a Unicorn-2 (right) (Source: [7])	7
2.5	MDQube-SAT (left) and a Hello Test satellite (right) (Source: [13][14])	8
3.1	An example of a rigid hinge used for spacecraft solar panels deployment (Source: Starsys Systems)	14
3.2	An example of a flexible hinge in its stowed (a) and deployed (b) positions (Source: [27])	15
3.3	The hinged system proposed by Kohla (2023) for PocketQubes (Source: [15])	15
3.4	Different types of HDRM mechanisms: Low-shock split spool (upper left), nichrome burn wire (upper right) and explosive bolt (down) (Sources: [31][30][32])	17
3.5	Bambu Lab X1 Carbon printer used to prototype the design (Source: Own elaboration)	18
3.6	Exploded view of Prototype 1 (Source: Own elaboration)	19
3.7	Deployed render of Prototype 1 (Source: Own elaboration)	20
3.8	Detailed view of the hinge system (Source: Own elaboration)	20
3.9	Exploded view of Prototype 2 (Source: Own elaboration)	21
3.10	Deployed render of Prototype 2 (Source: Own elaboration)	22
3.11	Mounting of the tape spring and hinge mechanisms (Source: Own elaboration)	22
3.12	Detailed view of the HDRM concept and configuration (Source: Own elaboration)	23
3.13	Exploded view of Prototype 3 (Source: Own elaboration)	24
3.14	Deployed render of Prototype 3 (Source: Own elaboration)	24
3.15	Final design of the HDRM mechanism, mounted onto the main box (Source: Own elaboration)	25
3.16	A pair of DIN 912 M2x8 screws used in the design (Source: Own elaboration)	26
3.17	Ruthex M2x4 threaded inserts (left) and APLI 0.35 mm Nylon Thread (right) (Source: [37][38])	27
3.18	Exploded view of the final design (Source: Own elaboration)	28
3.19	Image of the final mock-up (Source: Own elaboration)	28
3.20	3P assembly drawing, final design (Source: Own elaboration)	29

3.21 Selected resistance for the model (Source: [39])	30
3.22 Voltage effects on burning time and energy consumption (Source: Own elaboration)	31
3.23 Preliminary circuit design (Source: Own elaboration)	32
3.24 ANSYS Workbench simulations procedure (Source: Own elaboration)	33
3.25 Model preparation in ANSYS, with its coordinate system (Source: Own elaboration)	34
3.26 Model meshing (Source: Own elaboration)	35
3.27 Falcon 9 flight load limits (Source: [41])	35
3.28 Stress at the hinge region (Y Axis acceleration) (Source: Own elaboration)	37
3.29 Stress distribution with loads on the X axis (above), Y axis (center) and Z axis (below) (Source: Own elaboration)	38
3.30 Falcon 9 and Heavy frequency bin (Source: [41])	39
3.31 Natural frequencies obtained in the modal analysis (Source: Own elaboration)	40
3.32 Effective mass ratio for each mode and ratio (Source: Own elaboration)	40
3.33 Main modes deformation (Source: Own elaboration)	43
3.34 Sub modes deformation (Source: Own elaboration)	44
3.35 SMC-S-016 minimum random vibration environment during launch (Source: [43])	45
3.36 Random generated signal and its PSD, compared to the required PSD (Source: Own elaboration)	46
3.37 Image of the test setup, with the shaker, the model, and the accelerometer on the sliding backplate (Source: Own elaboration)	48
3.38 Measured signal and its PSD, compared to the required PSD (Source: Own elaboration) . . .	49
3.39 Top view of different configurations (Source: Own elaboration)	51
3.40 Side view of different configurations (Source: Own elaboration)	51
5.1 Representation of LEO population of satellites and debris. Most smallsats missions are orbiting in 350-700 km orbits, resulting in a rapid and safe de-orbiting after their mission lifespan (Source: [51][52])	54
6.1 Preliminary concept of a 3P design with double-hinged solar wings (Source: Own elaboration)	56

List of Tables

2.1	PocketQube external dimensions and sliding backplate dimensions for different number of units (Source: [5])	4
3.1	Ordered Weighted Average of the different alternatives (Source: Own elaboration)	10
3.2	Solar cell specifications (Source: Own elaboration)	11
3.3	Power outputs for different solar arrays configurations (Source: Own elaboration)	13
3.4	Resistance test results (Source: Own elaboration)	31
3.5	Mesh parameters (Source: Own elaboration)	34
3.6	ANSYS Structural Analysis Results (Source: Own elaboration)	36
3.7	Materials tensile yield strength (Source: Own elaboration)	36
3.8	Modal Analysis Summary (Source: Own elaboration)	41
3.9	Scalability feasability study (Source: Own elaboration)	50
4.1	Budget Summary (Source: Own elaboration)	52

List of abbreviations / Glossary

- **BOL/EOL:** Beginning Of Life / End Of Life
- **COTS:** Commercial Off-The-Shelf
- **HDRM:** Hold Down Release Mechanism
- **LEO:** Low Earth Orbit
- **OWA:** Ordered Weighted Average
- **Picosatellite:** Referred to a satellite between 0,1 and 1 kg.
- **PQ:** Short for PocketQube. Referred to a picosatellite standard where each P-unit has a size of 50x50 mm, and a mass of less than 250g.
- **PSD:** Power Spectral Density
- **ROSA:** Roll Out Solar Array
- **SF:** Safety Factor
- **SMA:** Shape Memory Alloy
- **TJ/QJ:** Triple-Junction solar cell / Quadruple-Junction solar cell
- **TLR:** Technology Readiness Level

Chapter 1

Introduction

1.1 Object

The HORUS team, which is part of the UPC Space Program, is developing missions based around the PocketQube standard and it will require a way to power the spacecraft that it intends to build. The objective of this project is to design, build and test a deploying system for foldable solar panels, that can be adapted for PocketQubes of 1, 2 and 3 P-units.

1.2 Scope

- To begin with, a literature review and state of the art of the folding and deployment mechanisms will be made, which will lead to a comparison and selection of the most suitable folding system.
- The structure will be designed in 3D using Solidworks. Further structural simulations using SolidWorks or similar software will be performed.
- The design will be subjected to modal analysis simulations in Ansys or similar software.
- The electronics and circuits of the deployment subsystem will be preliminary defined.
- The prototype will be 3D printed and assembled.
- The prototype will be subjected to vibration testing in order to ensure its compliance with launch regulations.

1.3 Requirements

- The deployment system shall be designed according to the PocketQube standards, and respect its size and volume requirements.
- The deployment system shall be designed to be adapted for 1, 2 and 3 P-units PocketQubes.
- The deployment system shall be designed to withstand vibration conditions during all mission phases.
- The deployment system will be designed in order to be easily built and assembled using COTS components.
- When deployed, the solar panels shall be able to produce enough energy to sustain the normal operations of the picosatellite.
- While deployed, the solar panels shall remain in a fixed unfolded position.
- While deployed, the solar panels shall be unable to return to its folded position.

1.4 Rationale

In recent years, the market of smallsats has experienced an exponential grow. Thanks to its reduction in cost, complexity and development deadlines compared to conventional satellites, along with a high accessibility and use of COTS, these platforms have grown beyond its initial educational and research purposes, and are now presented as an additional option for the New Space economic sector.

Along with this trend, the PocketQube standard has recently risen as a cost-effective and accessible window to space for universities and research projects. With 20% of the mass and volume of a CubeSat, this standard allows to launch and perform experiments and research for a fraction of the cost of a typical nanosat.

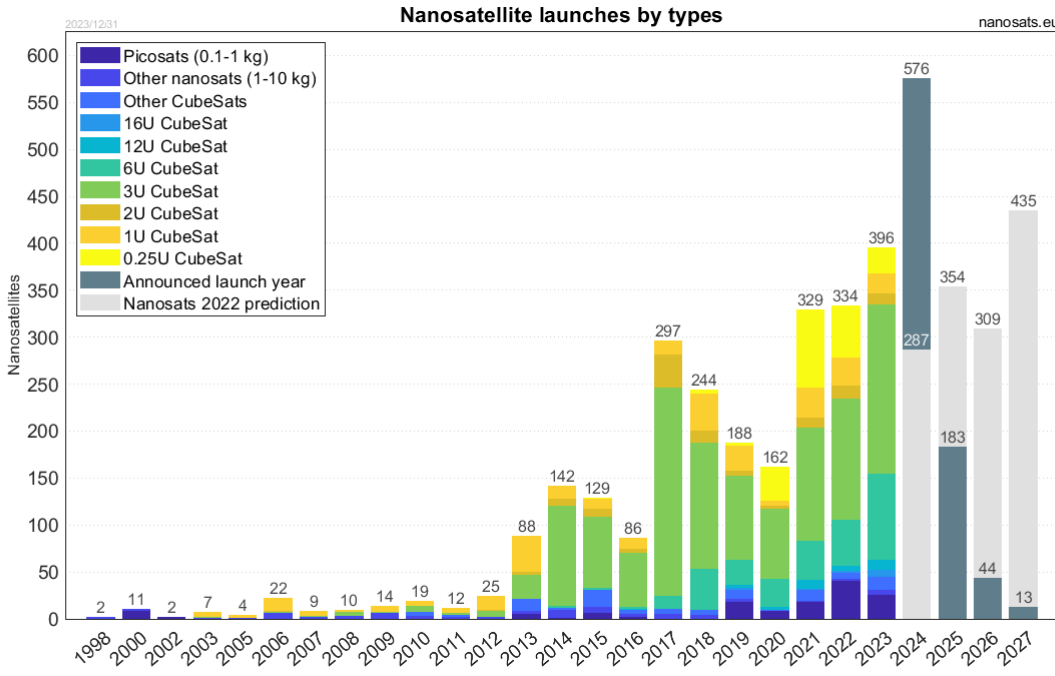


Figure 1.1: Nanosatellite launches by types (Source: [1])

As can be seen in Figure 1.1, picosatellites represent nowadays the 4% of nanosat launches. Anyway, its presence in low orbit is steadily rising, being the second most launched configuration after CubeSats, which often fall out of budget or dimensions for certain projects and users. Especially since 2021, the number of PocketQubes launched has increased noticeably, and this trend only seems to get stronger with each passing year.

However, PocketQubes are small, and many times they are limited by the amount of power their tiny solar cells can generate. Folding solar panels would increase the available area and power while maintaining the strict undeployed size standards that are typical of nanosatellites. For this reason, the development of a simple and effective deployment system would allow for more ambitious experiments, while maintaining the advantages of reduced cost launch and volume requirements. Therefore, this would solve one of the main drawback of picosatellites, and would position them as an even better option to access space.

Chapter 2

Review of the state of the art

2.1 The PocketQube standard

The PocketQube configuration was proposed back in 2009 by Robert J. Twiggs [2][3], although the first operative mission was not launched until 2013. That year, a Dnepr launcher vehicle lifted off from Yasny, Russia. One of the payloads was the UniSat-5 satellite [4], developed by Gauss Srl. Inside that satellite travelled the MRFOD demonstrator, which intended to deploy four picosatellites built following the PocketQube standard, in order to demonstrate the feasibility of this concept. Since then, more than 70 PocketQubes have been launched, with the cadence of launches beginning to increase as soon as 2021.

Since 2018, the PocketQube standard [5] has been regulated by TU Delft [6], Alba Orbital [7] and Gauss Srl [8], defining the requirements and constraints in order to design a picosatellite of this configuration. As stated in the introduction, the size of the PocketQubes is measured by P-Units. From 1P to 6P or more, each PocketQube is defined by these blocks, which measure 50x50x50 mm each.

Additionally, the deployment system makes necessary the use of a sliding backplate, affecting the final size of the satellite. The deployment mechanism makes use of a rail clamping system for the backplate, which maintains the satellite fixated to the deployer and guide it outside as smoothly as possible. Upon deployment, a spring inside the deployer push out the PocketQube, activating the kill switches on the way out and turning on the satellite electrical systems. Table 2.1 represents the changes in size of different configurations:

Table 2.1: PocketQube external dimensions and sliding backplate dimensions for different number of units (Source: [5])

Number of Units (P)	External dimensions without backplate (mm)	Sliding backplate dimensions (mm)
1P	50x50x50	58x64x1.6
2P	50x50x114	58x128x1.6
3P	50x50x178	58x192x1.6

2.2 Deployable solar panels in PQ

Since its beginnings, PocketQubes have not required large solar panels as its reduced volume meant an equally reduced power. For this reason, fixed solar panels were an elegant and simple solution to the power demands of these picosatellites. However, as the experiments and electronics inside the frame became more complex and energetically demanding, fixed solar panels began proving themselves inadequate and insufficient, especially with bigger configurations, like 2P and 3P PocketQubes [9].

As a result, a great number of 2P or superior PocketQubes (around and 80-85% of successful launches) have opted for deployable solar panels as its main energy captation system. However, 1P PocketQubes have not been affected by this trend and are still sticking to its fixed panel configuration, with only a 5% of the successful 1P launches using a deployable system. The total numbers of PQ launches with foldable solar panels can be observed in Figure 2.1, using the launch data from [10][1]:

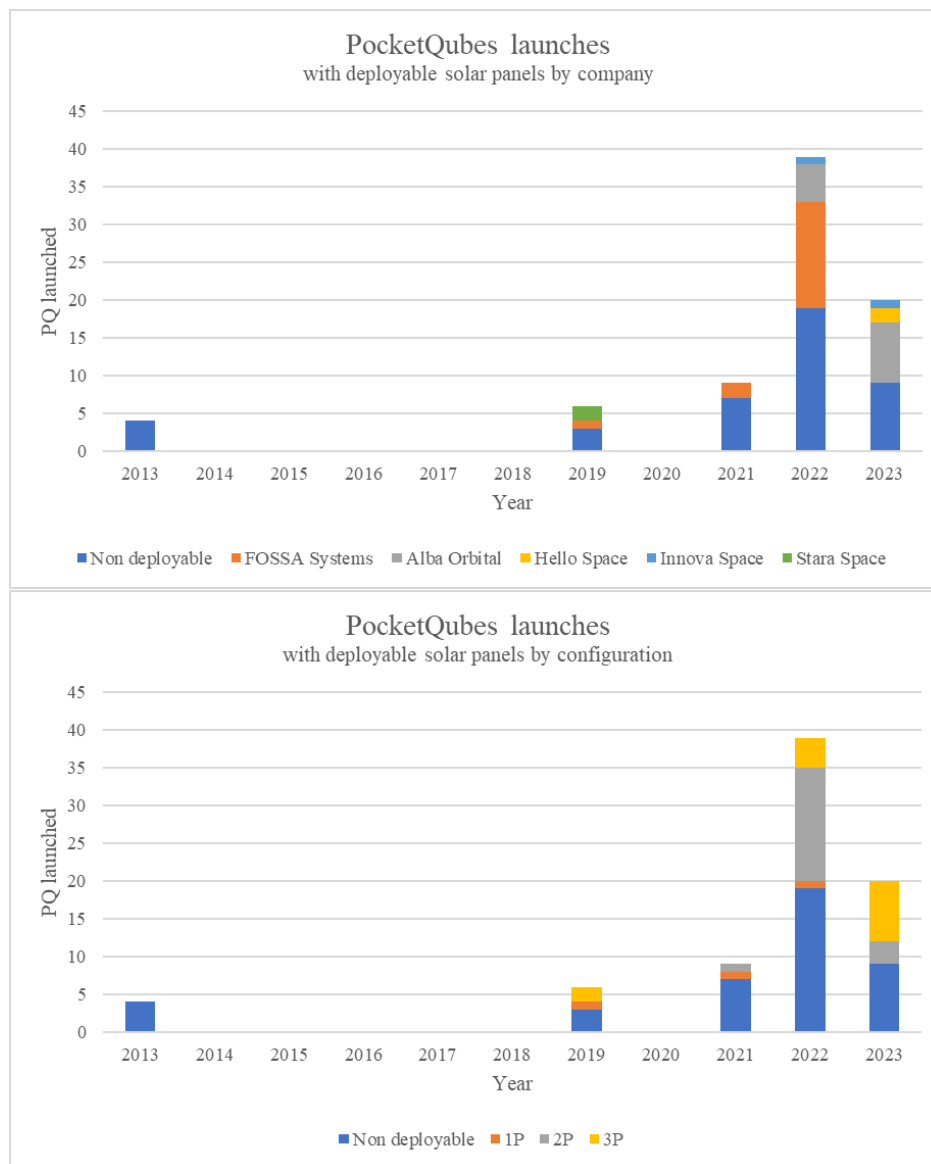


Figure 2.1: PocketQube launches with deployable solar panels since 2013 (Source: Own elaboration)

As the previous graph depicts, FOSSA Systems and Alba Orbital are the main figures in this field, with 17 and 13 deployable PocketQube launches in the last years, respectively. However, companies like Hello Space, Innova Space and Stara Space also launched picosatellites in this configuration, although in a much reduced rate. The proposals of each company will be discussed thoroughly later on.

Regarding deployable systems and appendages, the PocketQube standard [5] notes that the usual envelope for this components is assumed at 7 mm, although it could be increased to 10 mm in the case of larger deployers. As our PocketQube kit intends to be as accessible and practical as possible, it will be assumed an standard envelope of 7 mm. Figure 2.2 depicts the sizes of the components envelope:

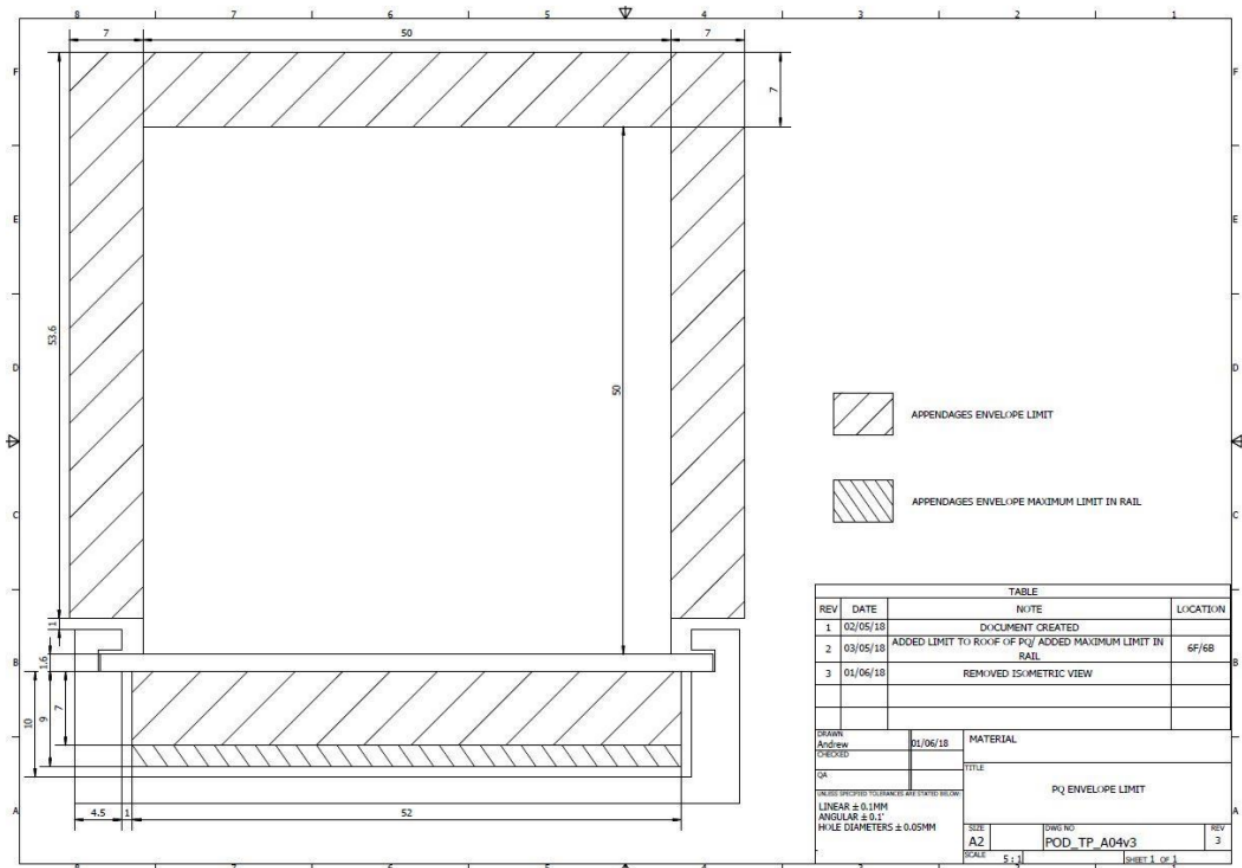


Figure 2.2: Components Envelope and Allowable Additional Envelope for Deployables (Source: [5])

Next, an updated state of the art of the sector of PocketQubes with deployable panels will be presented. Key players in this domain include FOSSA Systems [11], Alba Orbital [7], and others, who have launched numerous successful missions, demonstrating the practical applications and commercial viability of these small satellites. Their efforts, combined with ongoing research projects, continue to push the boundaries of what is possible in small satellite technology.

2.2.1 FOSSA Systems

FOSSA Systems [11], a spanish company dedicated to satellital telecommunications, developed and launched the first and still only successful 1P PocketQube with deployable solar panels, the **FossaSat 1**. It launched in December 2019 from New Zealand, on board of an Electron Rocket. The PocketQube featured four deployable Solarwings. A few years later, in 2022, a total of 14 **FossaSat 2E**, a 2P PocketQube with two triple-hinged Solarwings, were launched using a Falcon-9 rocket in two separate launches (Transporter 3 and 5).

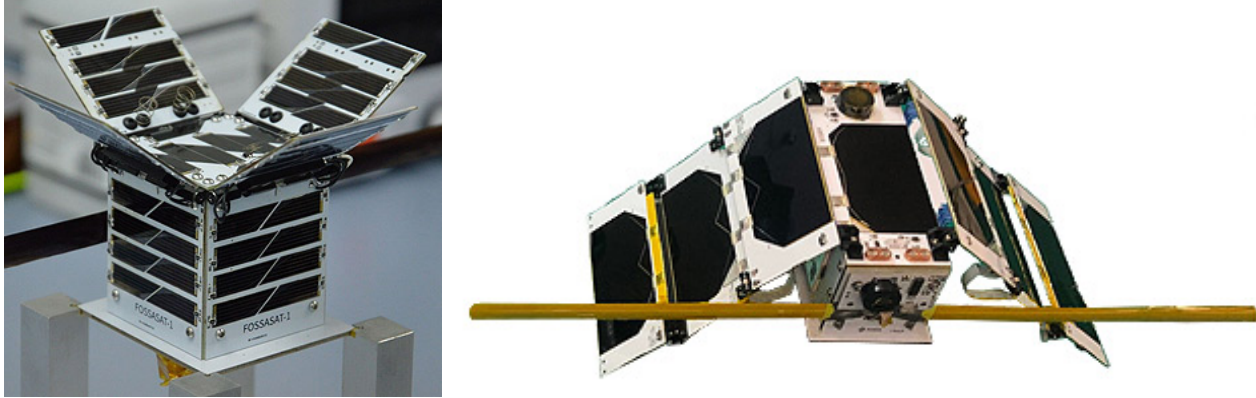


Figure 2.3: FossaSat-1 (left) and a FossaSat 2E (right) (Source: [11])

2.2.2 Alba Orbital

Alba Orbital [7] dedicates to sell PocketQube platforms in order to ease access to space at an unmatched cost respect other *smallsats*. They launched the **Unicorn-1** in January 2023 with the Transporter 3 mission. This 2P picosatellite featured four Solarwings deployed in a windmill shape. Later on, they developed the **Unicorn-2**, which will be used as a sellable platform in order to launch experiments at a competitive cost. As of 2024, 10 Unicorn-2 have been sucessfully launched, in the Electron "There and Back Again" mission, as well as in the Starlink 87, Korea 425 and Transporter 3 and 9 missions. This 3P has a set of two deployable panels in a four-hinged Solarwing configuration.

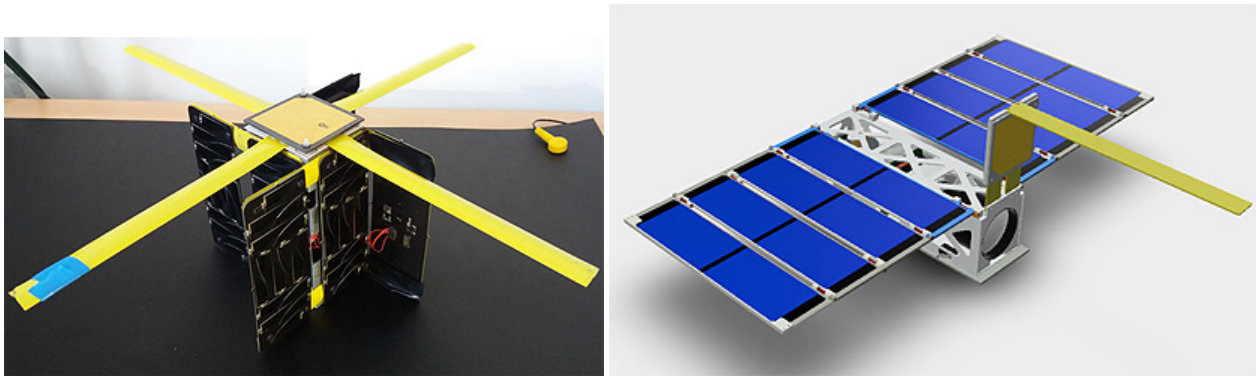


Figure 2.4: Unicorn-1 (left) and a Unicorn-2 (right) (Source: [7])

2.2.3 Other companies

Besides FOSSA Systems and Alba Orbital, other companies have developed and launched successfully PocketQubes with deployable solar panels. For example, Stara Space [12], based on telecommunication and *small sats* constellations, launched the **NOOR 1A & 1B** satellites back in 2019, with an architecture based on the aforementioned Unicorn-2 from Alba Orbital.

On the other hand, companies such as the argentinian Innova Space [13] developed its own platforms, like the **MDQube-SAT 1 & 2**, a 2P with two Solarwings. And Hello Space [14], for example, launched two **Hello Test** satellites, with a 2P form factor, as well as two triple-hinged Solarwings.

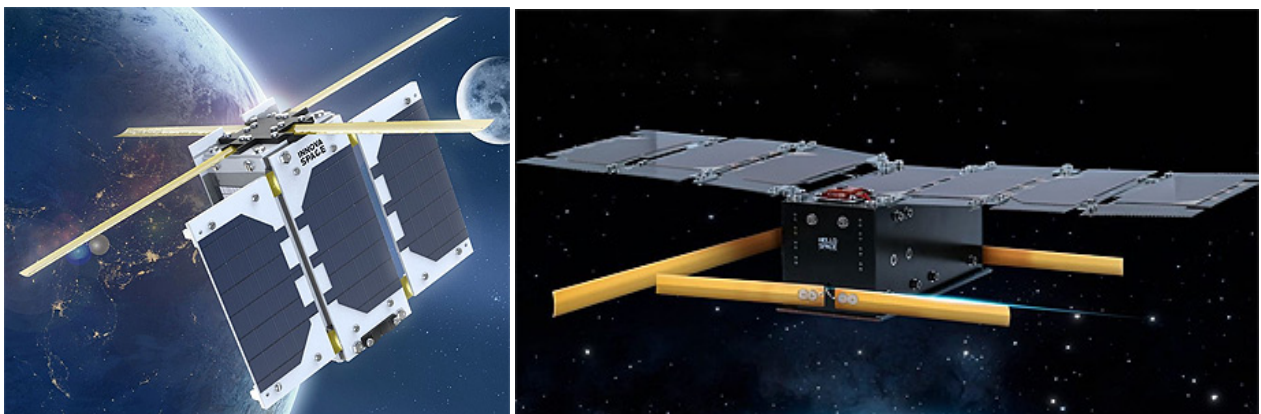


Figure 2.5: MDQube-SAT (left) and a Hello Test satellite (right) (Source: [13][14])

2.2.4 Research projects

Besides actual successful launches, a great majority of the knowledge and documentation related to the topic of this project can be found in research projects or articles. For example, the design document [15] for deployable Solarwings in a 2.5P, as part a R+D project in UPC ESEIAAT, is one of the main sources of documentation in this matter. This document is key and one of the few resources related to the deployable mechanism, so it would work as a base for the development of this project.

Additionally, other documentation like the UPMQube Proposal [16] or the 1P assembly document [17] from UPC will help to better understand the integration of the deployment mechanism from a systems engineering perspective, and how it relates to the rest of the components.

Chapter 3

Methodology

3.1 Folding mechanism selection

Regarding folding solar panels mechanisms in satellites, there is a wide range of options to choose from. Each one has its advantages and disadvantages, so a basic assessment will be performed in order to determine the most suitable option. For this matter, the ordered weighting average (OWA) method will be used.

In the space sector, we can differentiate the following types of folding mechanisms for solar panels:

- **Solar Wings:** This is the system used in all the PocketQubes launched to date, as seen in the previous section. The unfolding of the panels with a hinge system could be performed with accessible and COTS components. However, while its simplicity and reduced cost are its differential characteristics, it could also increase the vibrations after deployment, a phenomenon that should be studied in further testing. Additionally, this concept has a reduced volume and weight respect other alternatives, mainly due to its simplicity. Lastly, the effective surface could be increased easily adding more hinges to the assembly.
- **Sliding Wings:** This mechanism allows the solar panels to be deployed through a rail system. This method, although being slightly more complex and bulky, as well as reduce potential scalability to increase the effective surface, could also potentially reduce vibrations upon deployment. That is, it reduces the fluttering of the Solar Wing concept at the cost of some simplicity, weight, volume and scalability.
- **Origami:** This method stands out for both its complexity and great power generation. The folding of solar panels using origami would allow for a significant optimization in volume and effective surface. In fact, it has become a widely researched deployment method for space missions, where the optimisation of volume and weight is key [18]. Unfortunately, it has been considered that this method should fall out of scope due to the use of cutting edge materials and technologies, which would defeat the whole purpose of creating an accessible and cost effective design.

- **Rolled Wings:** The use of flexible solar panels such as the ROSA (Roll Out Solar Array) [19] panels at the International Space Station could also be considered for picosatellite applications, especially with the arrival of more cost effective alternatives to the public domain, such as the flexible GaAs cells from YimSpace [20]. However, due to the technical challenges and costs of such materials, along with the elevated design complexity of this type of configuration, it does not seem to comply with the design restrictions.
- **Solar Sail:** Lastly, the concept of a solar sail would reduce both volume and weight while increasing the potential power output [21]. Unfortunately, the elevated complexity and cost of this concept , along with a reduced technology readiness level (TRL) fail again to position this alternative as an attractive concept for our design.

So, after defining and weighting the most important features for our PocketQube design, based on the project requirements presented in Section 1.3, the OWA for each alternative would be as presented in Table 3.1:

Table 3.1: Ordered Weighted Average of the different alternatives (Source: Own elaboration)

	Weight	Solar Wings	Sliding Wings	Origami	Rolled Wings	Solar Sail
Cost (↓)	5	5	4	1	1	1
Power (↑)	5	3	3	4	4	5
Complexity (↓)	4	5	5	2	2	1
Weight (↓)	4	4	3	4	3	4
Volume (↓)	4	4	3	5	2	4
Scalability (↑)	3	2	1	4	5	4
OWA	25	3,92	3,28	3,24	2,72	3,12

As can be seen, the mechanism that is best suited for our design will be the hinged **Solar Wing** design, followed by the sliding wing and the origami configurations. It should also be noted that, as an additional advantage that was not taken into account in the OWA method, the Solar Wing design is far more documented and researched than its alternatives.

3.2 Solar cell selection

In order to select the most suitable option for the solar cells, three factors should be considered: an adequate size for a PocketQube standard, a space-graded component and, if possible, a good efficiency. The optimization of these parameters will provide the best option for this essential component. After a preliminary search, Azurspace [22] and Spectrolab [23] appear as the strongest commercially available options, due to its wide range of models and large production scale. For the sake of simplicity and COTS availability, no custom sized models will be presented. Additionally, certain cell types such as Silicon Cells will be excluded due to their lower efficiencies (below 20%) that would significantly increase the required surface area. The characteristics of the most suitable models are presented in Table 3.2:

Table 3.2: Solar cell specifications (Source: Own elaboration)

	Spectrolab		Azurspace	
Model	XTE-SF	XTJ Prime	3G30C	4G32C
Cell Type	Three-Junction GaAs			Four-Junction GaAs
Size [cm]	3.97 × 6.91		4 × 8	
Surface [cm ²]	27	27/26 ¹	30.18	
Efficiency (BOL) [%]	32.2	30.7	29.8	31.8
Efficiency (EOL) [%]	27.9	26.7	26.8	20.8

While being one of the most efficient models, the quadruple-junction QJ-4G32C cell from Azurspace will be discarded due to the high end of life (EOL) performance degradation, which would impair significantly the power generation capabilities of the PocketQube in the long run. Additionally, the Spectrolab models will be discarded as well for this project. This decision is purely related to the possibility of collaboration of these companies with the HORUS project, which is ultimately developing the PocketQube through this thesis. Due to the fact that Spectrolab declined any type of involvement in the project, the selected cell for this PocketQube will be the **Azurspace TJ-3G30C model**.

However, it should be stressed that, although discarding the Spectrolab models for specific logistic reasons purely related to our specific case, these alternatives should be seriously considered in similar projects.

¹Depending on a squared or a cropped corner configuration.

3.3 Power estimation

Once with the cell area and efficiency determined, the power generation of the satellite can be estimated using the following expression, extracted from Lason & Wertz (1999) [24]:

$$A_t = \frac{P}{S \cdot \eta} \quad (3.1)$$

where,

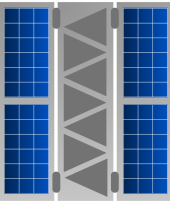
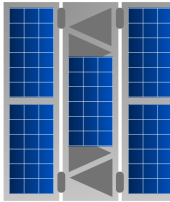
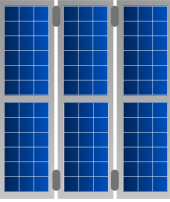
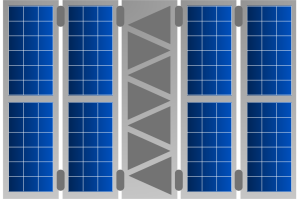
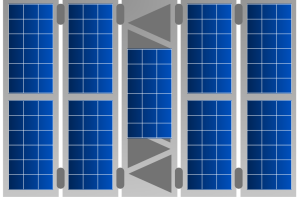
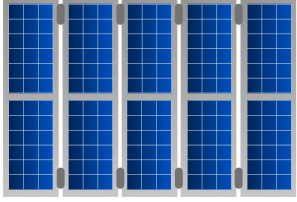
- A_t = Total surface area [m^2]
- P = Power [W]
- S = Solar constant [$\frac{W}{m^2}$]
- η = Efficiency

It should be stressed that the power estimation will be performed for the 3P configuration, as it is the most critical and complex assembly. Thus, given that the solar constant at Earth is about 1366 W/m^2 [25], and that the estimate efficiency of the solar cell is known, the needed area could be obtained for a required power requirement. However, the opposite could be done. Instead of obtaining the effective area as a result, different configurations could be presented, with the variable being the output power. Then, knowing that $A_t = n \cdot A$, being n the number of solar cells and A the area of each cell, the equation (3.1) could be manipulated into:

$$P = (n \cdot A) \cdot S\eta \quad (3.2)$$

Depending of the configuration, we would obtain the parameters shown in Table 3.3:

Table 3.3: Power outputs for different solar arrays configurations (Source: Own elaboration)

					
Cells	Surface [cm²]	Power [W]	Cells	Surface [cm²]	Power [W]
4	120.72	4.42	5	150.90	5.52
					
Cells	Surface [cm²]	Power [W]	Cells	Surface [cm²]	Power [W]
6	181.08	6.63	8	241.44	8.84
					
Cells	Surface [cm²]	Power [W]	Cells	Surface [cm²]	Power [W]
9	271.62	9.94	10	301.8	11.05

According to the power requirements imposed by the HORUS mission, the most suitable configuration would be the one with **6 solar cells**, providing a total power of **6.63 W**. This power generation is expected to cover all the critical subsystems of the PQ during the mission, as well as providing additional power for the payload.

Looking ahead into the future, an expanded version with 10 solar cells could be developed, increasing the total power generation to 11.05 W. This would significantly increase the variety and complexity of experiments that could be designed and mounted as a payload.

3.4 Hinge mechanism selection

The hinge mechanism is a crucial part for the deployment system, as it has to provide a safe and smooth opening process of the Solar Wings. The key feature of this mechanism is its ability to unfold the solar panels from its stowed position, and usually consist of three differentiate parts [26]:

- The mechanism responsible for the **deployment force** that moves the system from its stowed position.
- The **latching system** that keeps the assembly in its deployed position.
- The **delay or dampening** mechanism that avoids or reduce the locking shock and the possibility of the system to flap excessively or to bump into other elements of the spacecraft.

Based on these characteristics, hinged mechanisms are typically divided into two large groups: rigid and flexible hinges.

Rigid hinges, as can be observed in Figure 3.1, are usually formed by a pin joint, a pair of brackets, torsional springs which offer the deployment torque, as well as a latch and damper mechanism which can be added in order to minimize the locking shock. These hinges can be easily controlled and have a good performance, especially reducing the locking shock through advanced latching and dampening systems. However, this makes them complex, bulky and heavy, as well as increasing the cost of the components needed. Also, they need lubrication to work properly, which would significantly increase the complexity of the design, as well as its performance during its lifespan, as space-graded lubrications is usually costly.

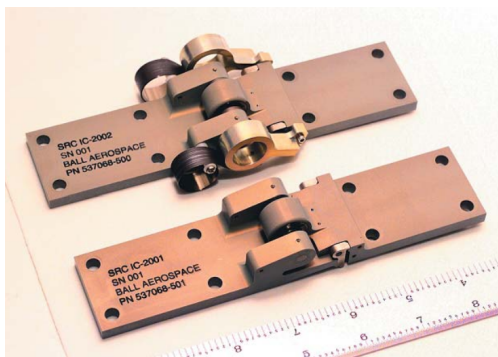


Figure 3.1: An example of a rigid hinge used for spacecraft solar panels deployment (Source: Starsys Systems)

On the other hand, **flexible hinges**, often called lenticular or carpenter tape hinges, are composed by two brackets and transversally curved strips known as tape springs, as shown in Figure 3.2. These tape springs are stowed in a buckled position, with a low bending stiffness. However, this stiffness increases when they are returned to their extended or pre-buckled state. In short, the torque generator and the latch mechanism are both implemented in the same component, the tape spring, through the use of elasticity. These systems, therefore, tend to be much more simpler, cost-effective and light respect to the rigid hinges. However, the performance of flexible hinges is usually lower, with a higher locking shock and a typically lower stiffness in the deployed position respect to fixed hinges.

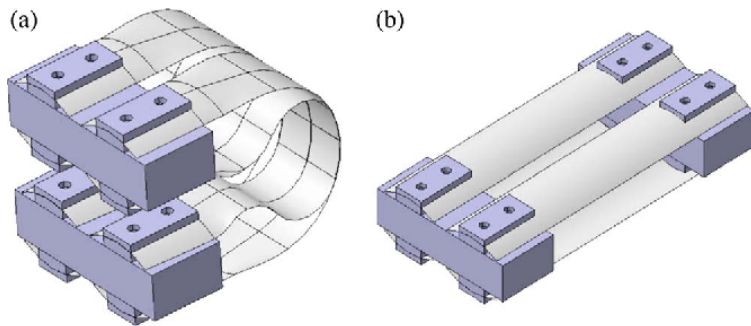


Figure 3.2: An example of a flexible hinge in its stowed (a) and deployed (b) positions (Source: [27])

Taking this into account, it seems clear that the most suitable option for the picosatellite will be the **tape spring hinge** mechanism. Due to this lightweight, cheap and simple configuration, this system complies with the requirements of the project. Regarding the state of the art, the mechanism could be developed from Kohla (2023)[15] design document, where the use of tape spring is complemented with rigid screwed hinges without spring force in order to maintain stability and compensate the lack of lateral stiffness of the tape spring mechanism. Although this design should be reviewed and improved (as stated in the design document itself) it is an excellent starting point for the design of the PocketQube. This configuration can be observed in Figure 3.3:

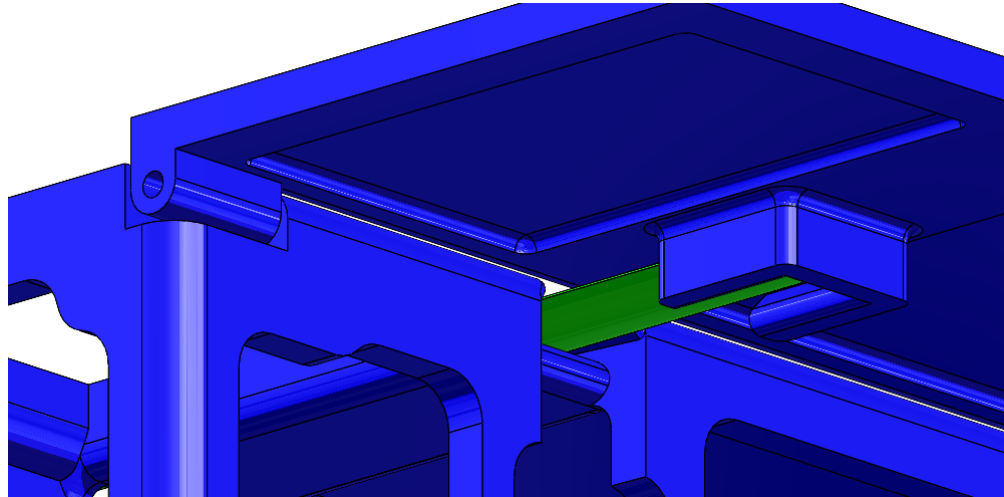


Figure 3.3: The hinged system proposed by Kohla (2023) for PocketQubes (Source: [15])

3.5 Hold Down Release Mechanism selection

The Hold Down Release Mechanism, also known as HDRM, is a key component of the assembly, as it maintains the satellite in its stowed configuration and, in a controlled way, allows the deployment of the system. For this purpose, several mechanisms and HDRM systems are used in the aerospace sector, some of which are briefly described below:

- **Pyrotechnic charges:** These are the most used HDRM mechanisms in conventional satellites. Through the regular use of explosive bolts that act like a latch (as seen in Figure 3.4), it ensures the safety of the system while inactive and provides a reliable deployment, with low maintenance and simple design. However, the shock waves produced by the explosion are propagated through the satellite. This can cause structural and electronic damage, especially to small satellites, which is why these mechanisms are being gradually replaced by low shock [28] or non-explosive alternatives.
- **Split spool mechanism:** The split spool is a mechanism conceived to replace explosive devices. This low-shock concept makes use of a tensile material and a spring loaded assembly that allows for the liberation of the bolt upon an electrical signal or a small explosion. This mechanism, although it can solve the disadvantages of the previous concept, it is very complex, heavy and large for small satellites, not to mention PocketQubes. An example of this configuration is also shown in Figure 3.4.
- **Shape memory alloys:** This mechanism takes advantage of the shape memory alloy (SMA) or muscle wire concept. These materials, which can be deformed at low temperature, return to their pre-deformed shape when applied heat, which is why they are regarded as excellent and simple actuators. Additionally, with the recent advancements in materials engineering allowing for higher temperatures to work with [29], these systems are becoming an interesting option for lightweight, small and simple HDRMs. Although this system would be ideal for a PocketQube (integrating the HDRM and the deployment mechanism in a single component), these materials are not cheap or commercially available at the moment. For example, the most famous SMA, Nitinol, is an alloy made from nickel and titanium, materials known for its scarcity and elevated cost.
- **Burning wire:** Lastly, the burn wire mechanism is a great option for the scope of the project due to its simplicity, low cost and lightness. This systems keeps the components in a stowed position through threads, usually Nylon. These threads are maintained in contact with an electrical resistance or a nichrome wire [30]. In order to trigger deployment, an electrical current is passed through these components, burning the Nylon wire and releasing the assembly. Despite its obvious advantages, this mechanism lacks the reliability of other systems, which is why is it usually designed with redundancy.

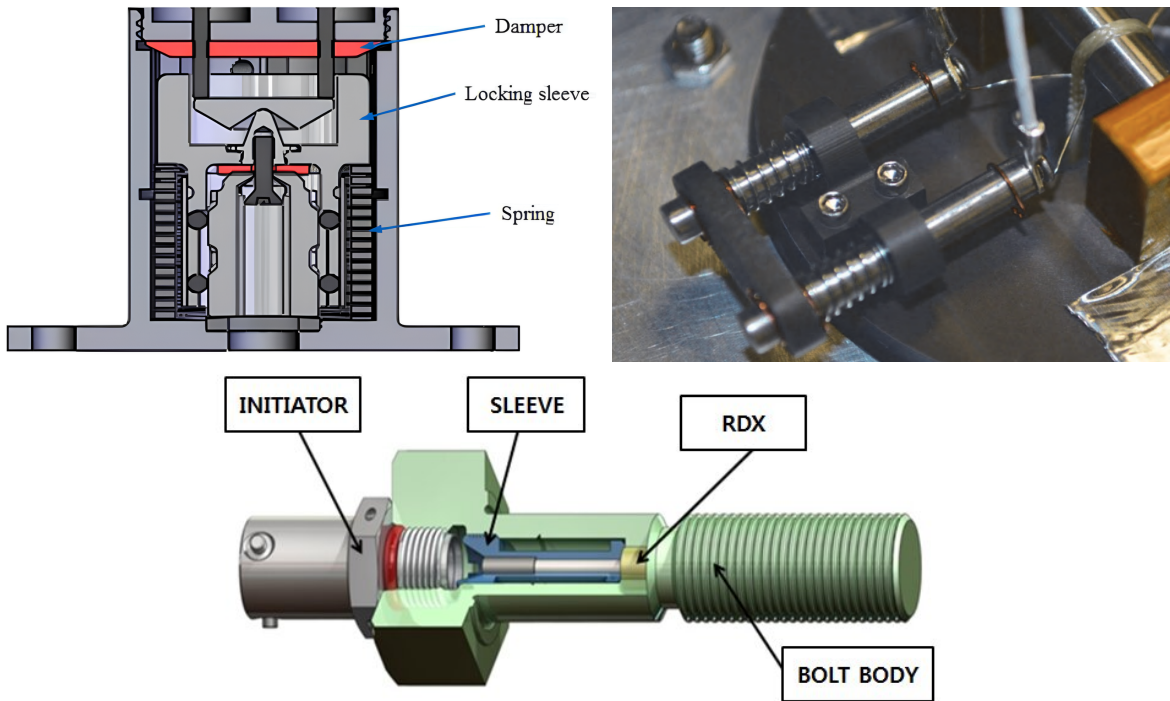


Figure 3.4: Different types of HDRM mechanisms: Low-shock split spool (upper left), nichrome burn wire (upper right) and explosive bolt (down) (Sources: [31][30][32])

After reviewing the different options, it seems clear that the **burning wire** configuration is the most adequate design for our PocketQube, as it meets all the requirements of the scope. Its simplicity, low cost and reduced weight make it an excellent choice for this project. However, reduced smoothness and reliability will be its main drawbacks, which should be addressed through redundancy and smart design.

Regarding this HDRM mechanism, several variations can be found based around the concept of burning a wire through electrical current. Besides the already mentioned nichrome burn wire, depicted in Figure 3.4, the use of pogo-pins and a burning resistance [33], used for cutting a nylon thread, could also be an interesting solution in order to maximize the use of COTS components in the assembly. However, the final characteristics of the HDRM mechanism will be determined during the design phase of the project.

3.6 Structural design

Once with the design concept closed and all the systems defined, the next step is to implement these features into a 3D model. For this purpose, SolidWorks will be used for the structural design. The design will follow an **iterative approach**, taking advantage of the 3D printing capabilities of the HORUS mission. For this reason, several prototypes will be printed, inspected and verified, gradually testing all the design features and refining the design up to the final model, which will be the one to be experimentally tested. It should be stressed that all the prototypes are based on the 3P configuration, as it is considered the most critical design. Scalability to other configurations will be discussed in latter sections.

All the prototypes were printed in PLA using a **Bambu Lab X1 Carbon** [34], a filament 3D printer with a nozzle precision of 0.2 mm. The printer setup can be observed in Figure 3.5



Figure 3.5: Bambu Lab X1 Carbon printer used to prototype the design (Source: Own elaboration)

3.6.1 Prototype 1

The objective of the first prototype was mainly to develop the basic frame of the PocketQube according to its standards [5], as well as making sure that the printer settings and precision complied with the expected tolerances and general measurements required. Additionally, this prototype was key in order to mount the model for the first time, thus verifying the fitting of all components and the general rigidity of the assembly.

As can be seen in Figure 3.6, the main components of the assembly are the following ones:

- **Main box:** As the PocketQube main structure, it serves as a housing for the payload, batteries and electronics. The slots for the hinges were added and integrated into the general structure, and the

topological design was intended to keep the structure lightweight but rigid and resilient. The top of the main box was designed in order to fit one solar panel, a characteristic that would later change to comply with the design concept.

- **Sliding backplate:** The sliding backplate design was at this time very simple, with the main objective of testing the tolerances of its mounting to the main box, through four L-shaped pins that snap fitted into the main box.
- **Solar wing:** Finally, the solar wings and its hinges were designed in order to maintain the size of the PocketQube below the envelope maximum (as defined by the standard seen in Figure 2.2), while having the necessary surface for two solar panels each. The hinge mechanism, based on the one proposed by Kohla & Kuijjer [15], was improved based on the feedback proposed in the original design document. To reduce the bending of the solar wings, the hinges were moved to the center of the assembly. Additionally, it was designed with four screws per solar wing, with the bolts being mounted on the interior part of the hinge, avoiding the problem of bolt heads sticking out of the envelope.

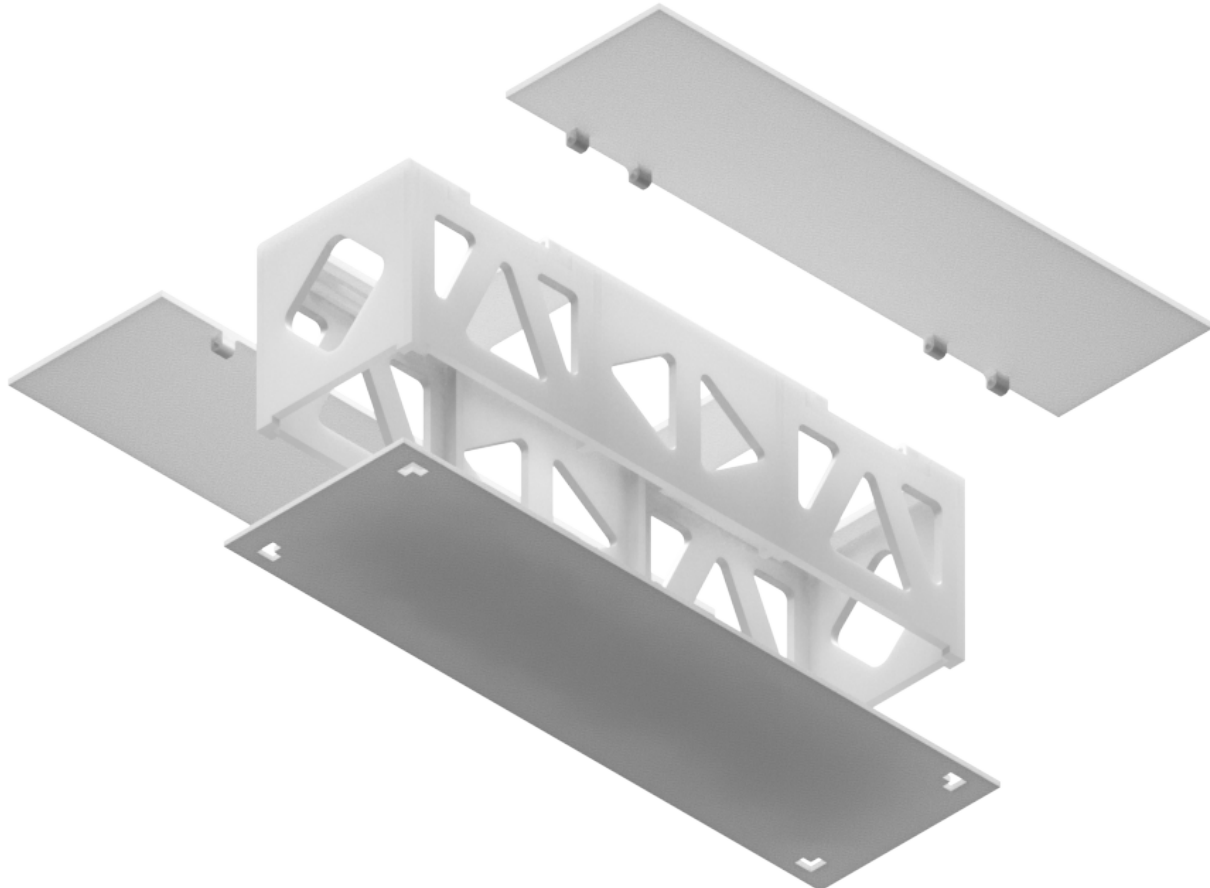


Figure 3.6: Exploded view of Prototype 1 (Source: Own elaboration)

Although the prototype was considered satisfactory, some improvements were taken into account for future iterations. The main ones are described next, along with some detailed renders in Figures 3.7 and 3.8:

- The attachment of the sliding backplate to the main box was not perfect, and it usually bent significantly. It was decided to add more pins to reduce this problem, as well as designing a bolted mounting system for more advanced prototypes.
- Bending problems also appeared on the solar wings. Although not being of great significance, the solar wings did not seem very robust, mainly due to their thinness. It was decided to increase the printing infill in this particular component (using a 2D honeycomb pattern, and increasing the infill density from 15 to 30%).
- Minor changes to measurements and tolerances were implemented in order to make the mounting smoother.

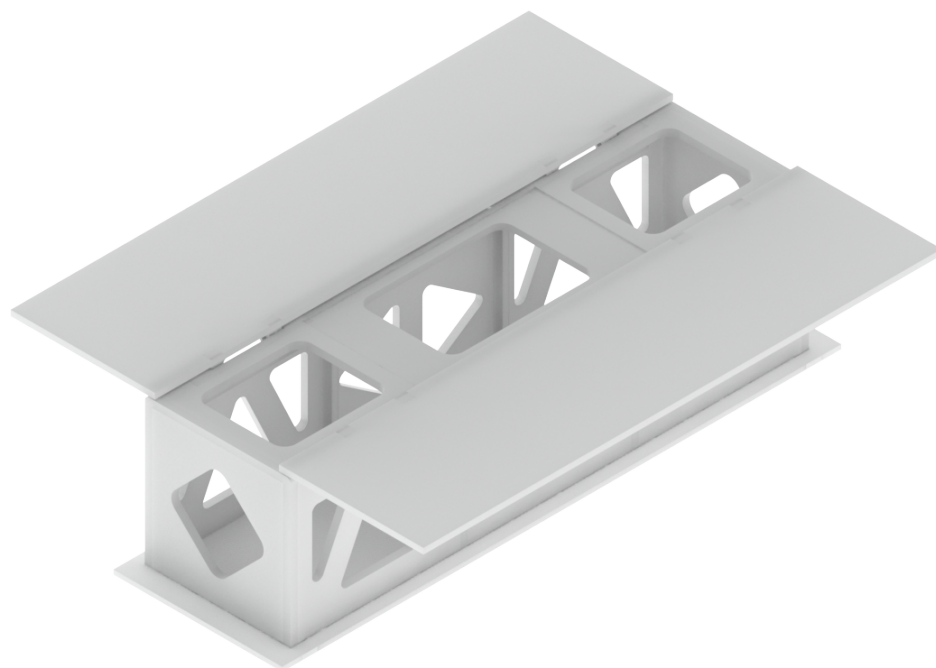


Figure 3.7: Deployed render of Prototype 1 (Source: Own elaboration)

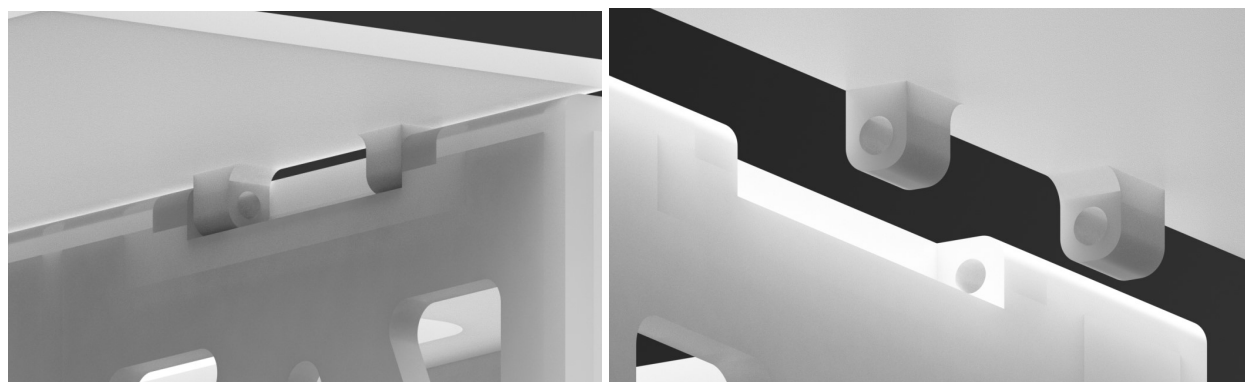


Figure 3.8: Detailed view of the hinge system (Source: Own elaboration)

3.6.2 Prototype 2

With the main frame and mounting procedure verified, the designing of the second prototype focused on testing the tape spring and hinge system. Testing the stiffness of the tape spring, as well as ensuring a smooth release and reduced slack, were the main objectives for this prototype.

The main changes respect the previous iteration were the addition of the tape spring slots, improvements in the design of the sliding backplate, as well as a redesign of the central wall of the main frame. Additionally, multiple adjustments and minor changes were introduced to improve tolerances, reduce slack and increase smoothness and easiness of mounting. The render of this prototype can be seen in Figure 3.9, with the aforementioned changes:

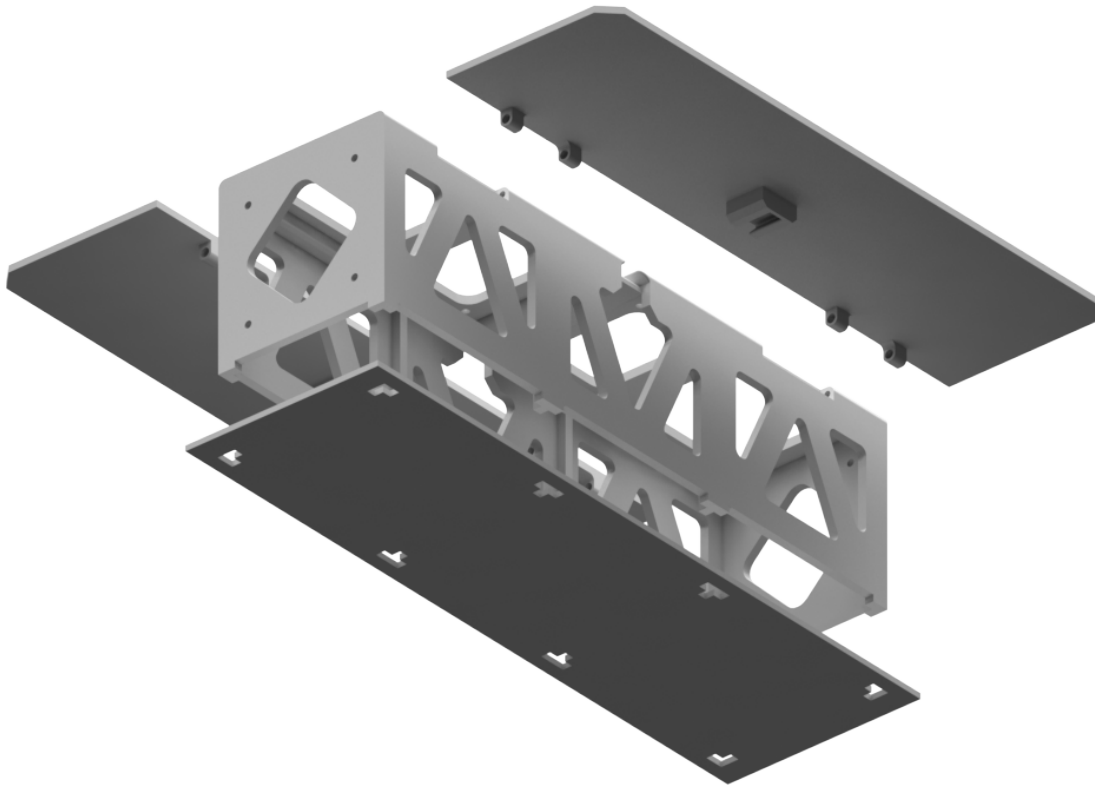


Figure 3.9: Exploded view of Prototype 2 (Source: Own elaboration)

This design proved to be a complete success. The tape spring along with the hinged mechanism worked nicely, with enough strength to deploy the solar wing with ease. Each tape spring measured 8 mm in width, and was easy to mount. Further tests verified excellent fatigue behaviour, as the tape spring maintained its force after long periods of time in a stowed position.

Additionally, the system was designed in order to be easily mounted. Using a total of 8 DIN 912 M2 bolts, and a tape spring, it is possible to quickly build the complete deployment mechanism with everyday tools. Further testing will determine its behaviour under launch conditions, however, at this point, the design was considered successful and the prototype was verified. The prototype is depicted in Figures 3.10 and 3.11. Nevertheless, some improvements were noted for future prototypes, for instance:

- The central main frame needed rework for future scalability concepts (see Section 3.10)
- The top of the main box needed a modification in order to include an additional solar panel.
- Modification in the tape spring slots, making them thinner in order to reduce slack.

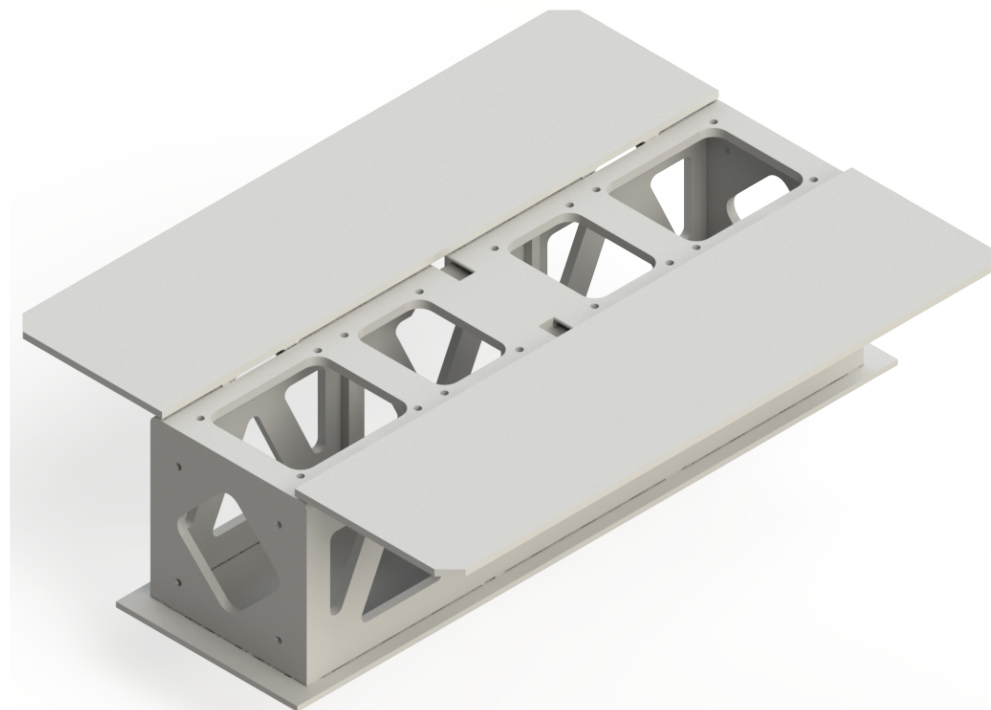


Figure 3.10: Deployed render of Prototype 2 (Source: Own elaboration)

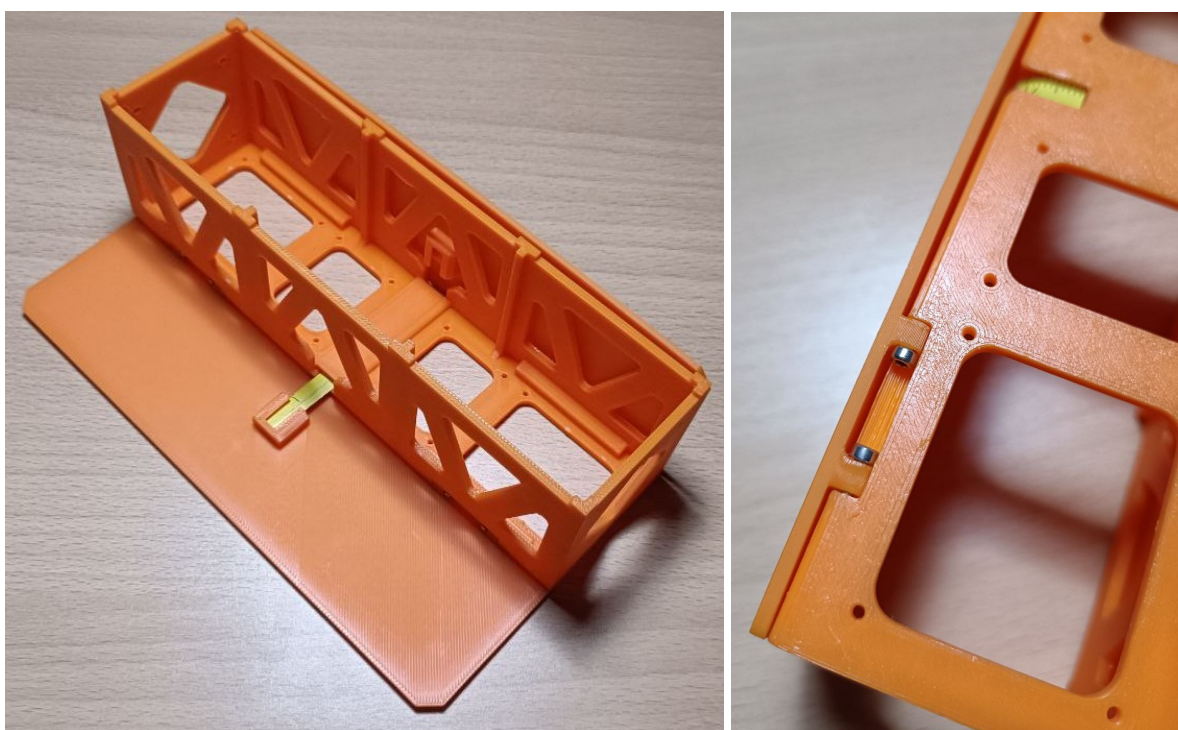


Figure 3.11: Mounting of the tape spring and hinge mechanisms (Source: Own elaboration)

3.6.3 Prototype 3

The objective of the third prototype was, among other things, to design and test the HDRM subsystem, based on the burning wire configuration. However, it also tested the new sliding backplate fixation system, as well as a refined design for the tape spring slots.

The HDRM design involved an integrated structure into the sliding backplate to tighten the nylon thread around it. Additionally, holes were added to the solar wings in order to pass the threads, thus creating a rigid and simple HDRM mechanism. As can be observed in Figure 3.12, the burn resistor was designed to be placed on the sliding backplate structure. As a preliminary design, the resistance is planned to be placed with no additional support, but the final product should have a dedicated electronic board mounted onto the support to secure the resistor, as well as to reduce weight and volume.

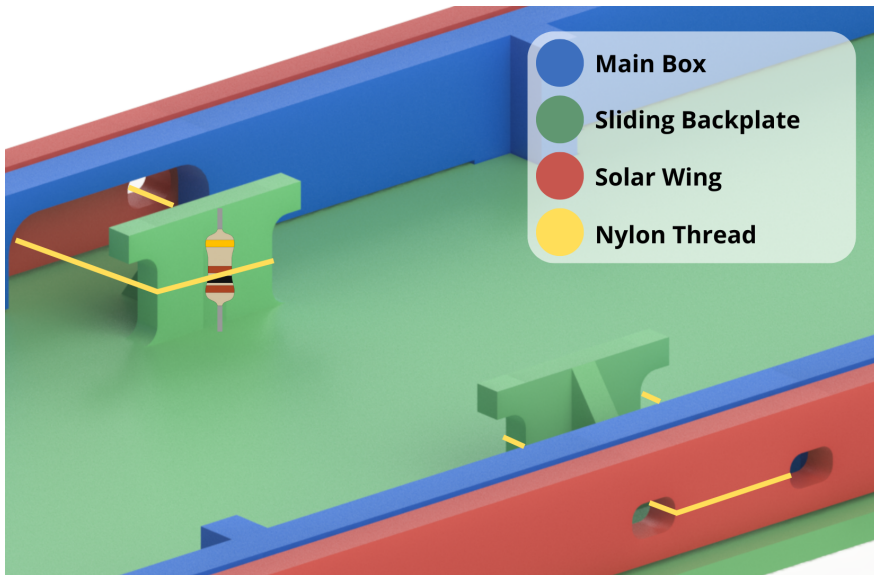


Figure 3.12: Detailed view of the HDRM concept and configuration (Source: Own elaboration)

Additionally, the new sliding backplate fixation included four M2 bolts that were screwed to the main frame through inserts. This allows for a simple and rigid union that complements the snap fit pins at the middle of the backplate. Detailed renders of this ptototype are depicted in Figures 3.13 and 3.14.

This iteration, however, did not perform as well as expected, due to the following reasons:

- The HDRM design, although feasible, was very difficult to mount and it was decided to modify it for the sake of simplicity. This was due to the fact that it was mounted on the sliding backplate, which meant that the nylon thread would need to be assembled with the PocketQube closed. This proved to be an almost impossible task, so it was decided to implement the design on the main frame.
- The design changes implemented in the tape spring slots and deployment mechanism tolerances in order to reduce slack, did not change the smoothness of the deployment. In fact, it made more difficult the assembly mounting, so it was decided to revert to the original design of Prototype 2.
- Some non-compliances respect the PocketQube standard [5] were found in the design. Specifically, the

solar wing span in its stowed position exceeded the envelope defined in Figure 2.2. Luckily, the redesign would not affect the performance of the model, so this change would be applied in future prototypes.

- Although it did not affect the performance of the design, an additional HDRM system for redundancy was recommended in order to increase the safety and reliability of the design. This redundant HDRM would be placed around the PocketQube, and would prevent it from deploying inside the deployer in case that the individual HDRMs failed.

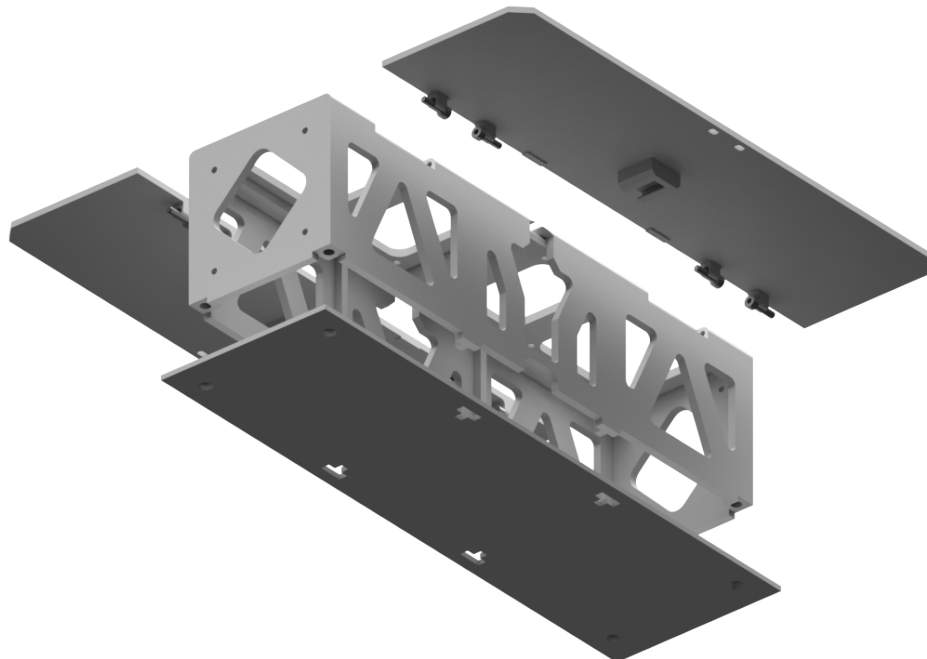


Figure 3.13: Exploded view of Prototype 3 (Source: Own elaboration)

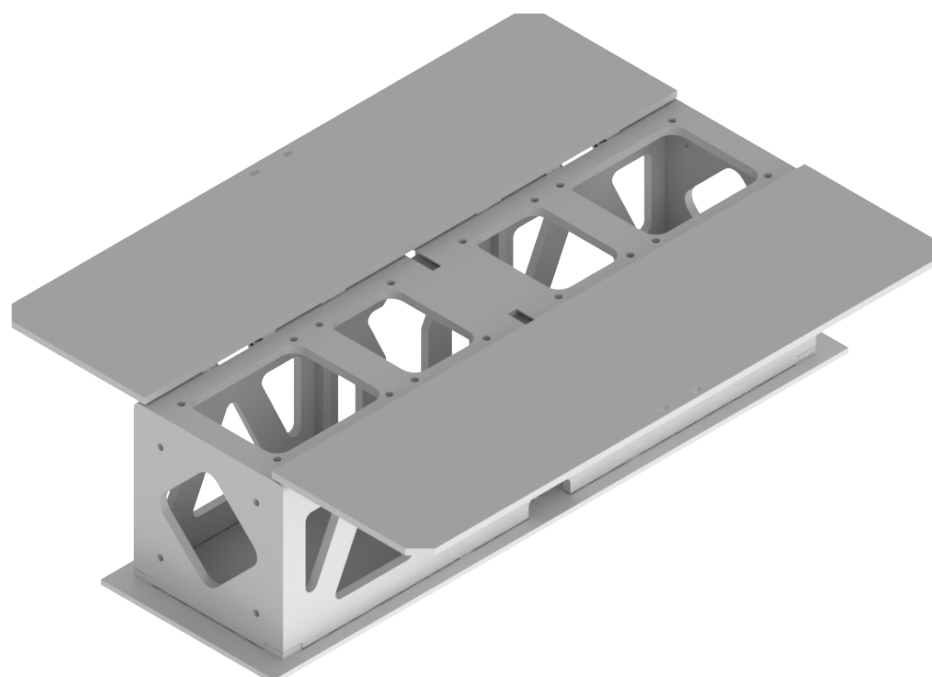


Figure 3.14: Deployed render of Prototype 3 (Source: Own elaboration)

3.6.4 Final design

The final design is the result of all the prototype iterations, a process that could not be possible without the iterative capabilities of the project given by the accessible 3D printing tools which allow for quick and adaptative prototyping. As this is the final design that will be tested, the main subsystems will be presented in its final configurations.

- **Main Box (3PQ-M-001):** The main box, in its final design, is the most complex and critical piece of the assembly. Made from one piece, it has multiple purposes: the housing of the electronics and components in a structural and rigid structure that complies with the PocketQube standards [5], as well as the integration of the hinge, deployment and HDRM subsystems in its design, as depicted in Figure 3.15.

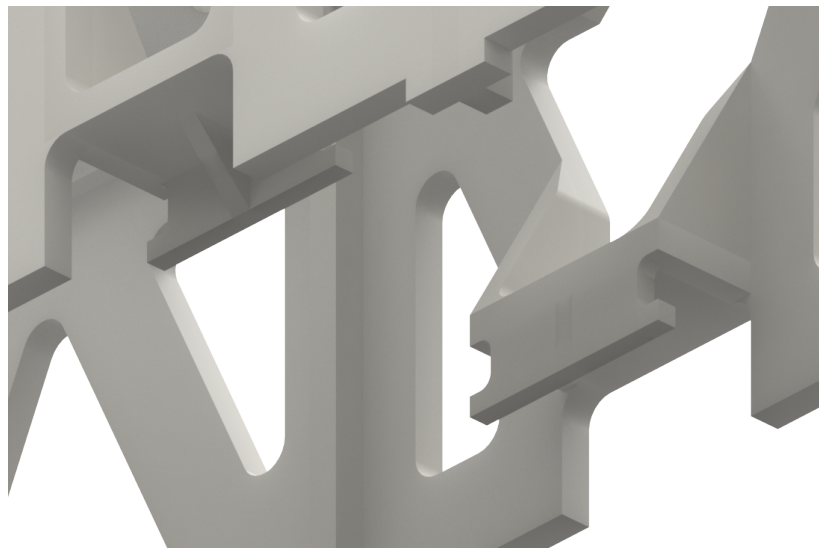


Figure 3.15: Final design of the HDRM mechanism, mounted onto the main box (Source: Own elaboration)

- **Sliding Backplate (3PQ-M-002):** The sliding backplate has the key objective of allowing the fixation and deployment of the satellite. Thus, it must ensure a safe and strong fixation to the main box, which has been done through the use of bolted unions and snap-fit pins. Additionally, the sliding backplate complies with the aforementioned standards.
- **Solar Wing (3PQ-M-003):** Finally, the solar wing is the differential characteristic of this design respect similar PocketQubes. Through a tape spring attached to the main box, as well as the hinged subsystem, the solar wings are designed to deploy effectively and safely. Moreover, the HDRM mechanism integrated in the main box ensures that the solar wings remain stowed during launch and before deployment, including redundancy mechanisms in case of failure. At the precise moment, an electrical current through the HDRM circuits is designed to burn the nylon thread that prevents deployment. Once deployed, this configuration allows the power output to increase around 600% respect other PocketQubes with fixed solar panels [35].

For the assembly of the final design, beyond the PLA structure, other components have been used. As stated at the beginning of the report, the objective of this project is to develop a functional but simple and cost-effective design that can be printed and mounted with COTS components and day to day materials. In this aspect, the additional materials used for the design assembly are the following ones, also shown in Figure 3.17:

- **Tape Spring:** As stated in Section 3.4, the tape spring mechanism allows for a simple and reliable configuration that takes advantage of the material properties of tape spring, thus avoiding any kind of powered system. In the case of this design, a 9×32 mm tape spring has been used for each Solar Wing, cut from a generic COTS tape spring in order to fit the slot.
- **Bolts:** The bolts selected for the design have been the **DIN 912 M2** standard (depicted in Figure 3.16), made of 304 Stainless Steel [36]. The DIN 912 standard, with its hexagonal socket head configuration, has been selected for its reliability, versatility and wide availability. Additionally, the metric M2 has been chosen for its reduced volume while being an abundant COTS component that can be easily purchased.



Figure 3.16: A pair of DIN 912 M2x8 screws used in the design (Source: Own elaboration)

- **Inserts:** The use of threaded inserts has been crucial to ensure the attachment between the sliding backplate and the main box. Unlike the solar wing hinges, which are supposed to be mounted only once, the sliding backplate is designed to be mounted and removed multiple times in order to access the interior of the PocketQube. For this reason, a simple bolt screwed directly into the PLA was not a feasible concept as the repeated use would cause slack and fatigue. Threaded inserts are a simple and elegant solution to this, and for this case, four M2x4 Ruthex brass inserts [37] were added to the main box. These components are specially designed for 3D printed materials, being inserted by heat. Their wide availability and low cost makes them an effective and suitable option for this design.
- **Nylon Thread:** Lastly, a 0.35 mm Nylon thread [38] was used for the HDRM mechanism. This material was selected for its cost-effectiveness, its reduced weight and great strength. Additionally, Nylon is a non-conductive material, and with a range of burning temperatures that allow for a burning wire configuration (see Section 3.7).



Figure 3.17: Ruthex M2x4 threaded inserts (left) and APLI 0.35 mm Nylon Thread (right) (Source: [37][38])

Next, a render of the final design is depicted in Figure 3.18, as well as an image of a printed design with fake solar cells in Figure 3.19, simulating the final aspect of the model. As can be seen, all the mentioned changes have been implemented, as well as the needed screws. Additionally, in the following page, a general blueprint of the assembly is provided (Figure 3.20). It should be noted that, for the sake of brevity, the final blueprints of the individual assembly components are also provided in the respective Blueprints Annex.

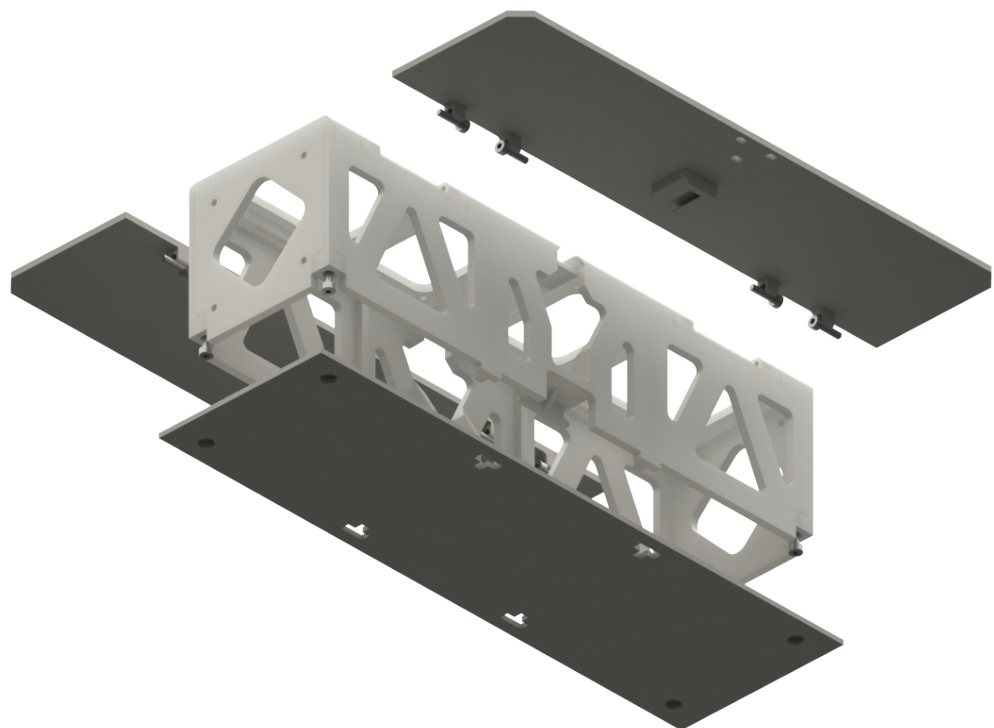


Figure 3.18: Exploded view of the final design (Source: Own elaboration)

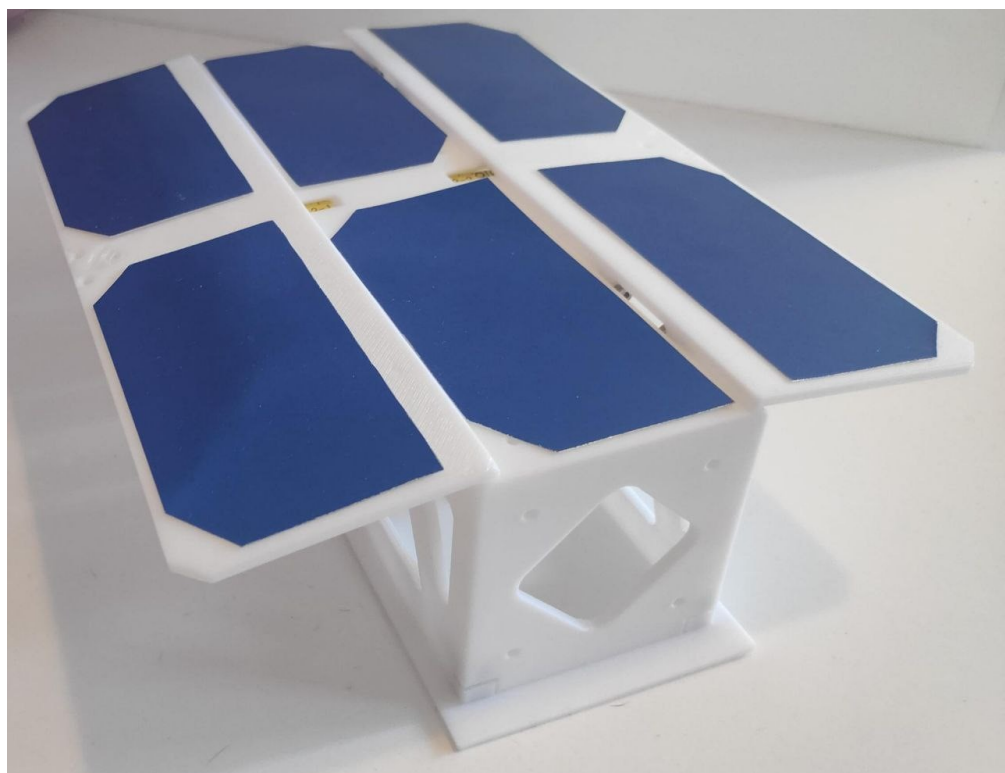
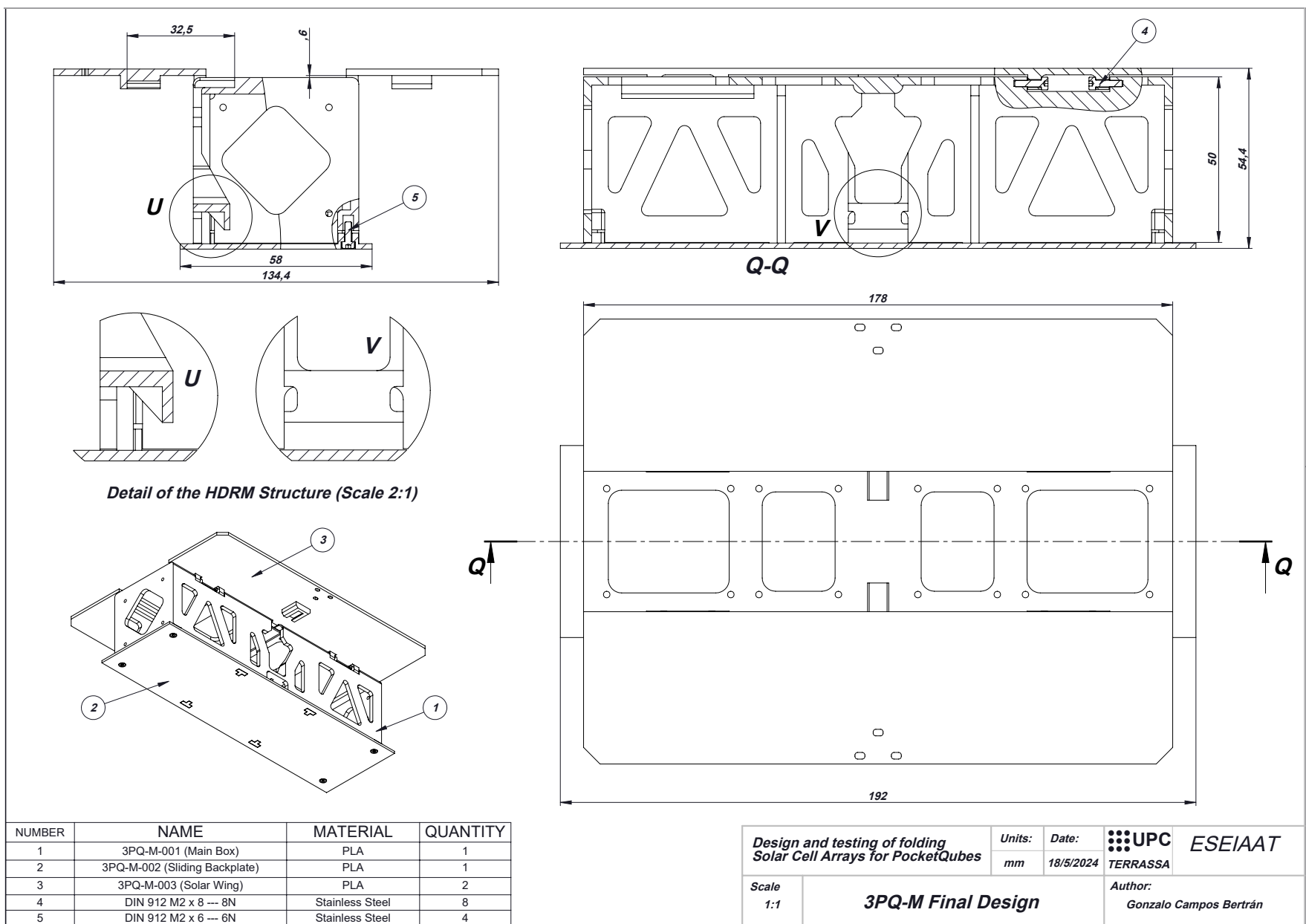


Figure 3.19: Image of the final mock-up (Source: Own elaboration)

Figure 3.20: 3P assembly drawing, final design (Source: Own elaboration)



3.7 Electrical design

For the scope of this project, the preliminary design of the electrical subsystem is intended only for the HDRM mechanism. The concept defined at Section 3.5 and structurally designed in the previous section includes, as can be seen in Figure 3.12, a Nylon thread in contact with a resistance. Each resistance and thread assembly help to keep each Solar Wing in a safe stowed position. Additionally, as previously mentioned, a third resistance and thread has been added around the model, in order to increase the reliability of the system in its stowed configuration during the launch.

3.7.1 Components selection

For the selection of the resistance, it is important to find a component that can be burnt and cut the wire with a low electrical current, while being cost-effective and widely commercially available. According to Ohm's law:

$$P = RI^2 \implies I = \sqrt{\frac{P}{R}} \quad (3.3)$$

So, in order to minimize the current, it is important to select a resistance with low nominal power. Additionally, an increase in resistance will further lower the current, at the expense of elevating the voltage. The best option is to find a component that allows to reach nominal power with neither extreme current or voltage. For these reasons, the selected resistance, as shown in Figure 3.21, has been a simple **100Ω resistance** with a nominal power of **0.25W**.



Figure 3.21: Selected resistance for the model (Source: [39])

In order to characterize the energy consumption of this subsystem, a series of tests have been conducted on these resistances in order to determine the precise combination of voltage and burning time that optimize the behavior and meet the requirements. The results can be observed in Table 3.4:

Table 3.4: Resistance test results (Source: Own elaboration)

Voltage (V)	Power (W)	Time (s)	Energy (J)
8	0,73	30,0	21,90
9	0,91	20,0	18,20
10	1,10	10,0	11,00
11	1,32	5,0	6,60
12	1,59	4,8	7,63
13	1,87	5,0	9,35
15	2,60	2,2	5,72
20	4,60	1,0	4,60

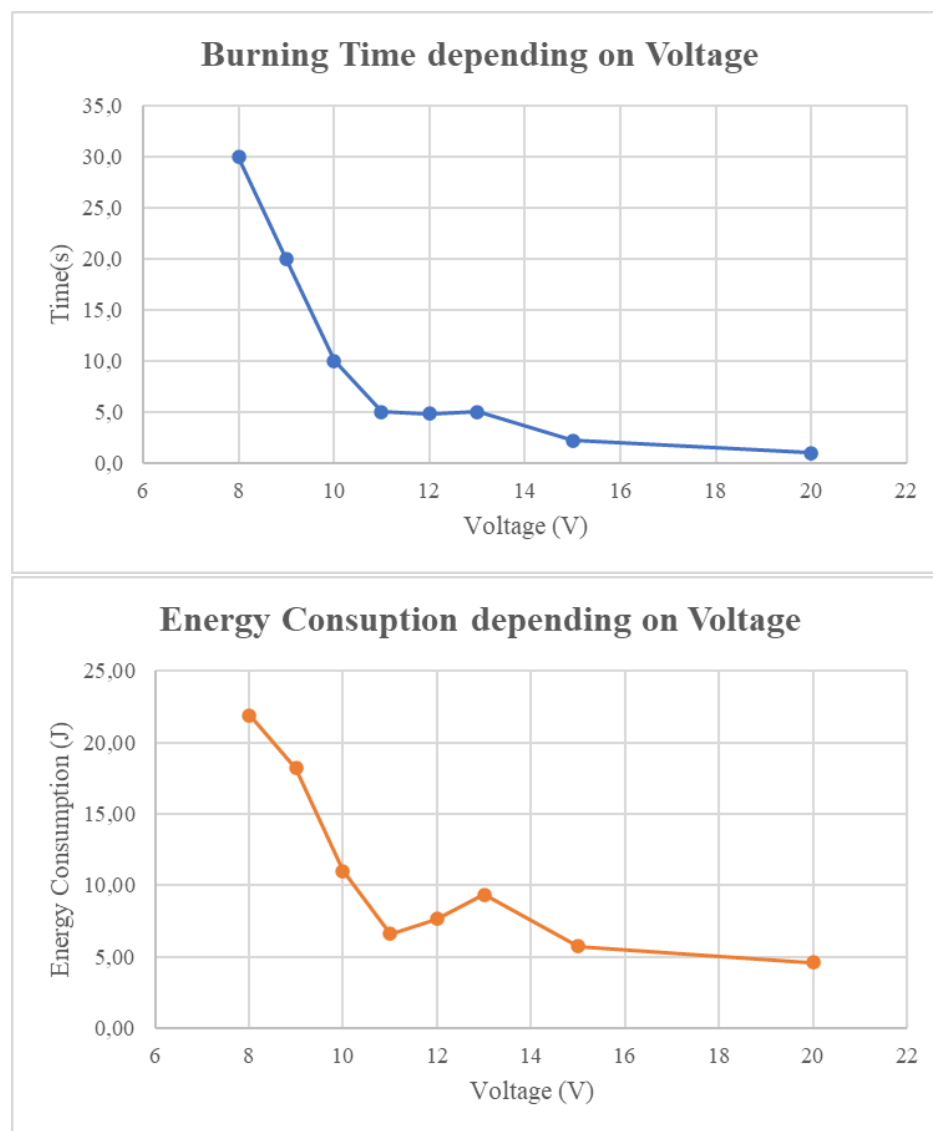


Figure 3.22: Voltage effects on burning time and energy consumption (Source: Own elaboration)

As can be observed in Figure 3.22, the burning time is reduced fairly exponentially with an increase in voltage. It should be noted that, although the nominal power of the resistance is 0.25W, the heat produced from overloading the resistance is not sufficient to burn the Nylon thread until a power of around 0.75W has been achieved (which represents three times the nominal value). Additionally, the burning time seems to flatten at around 1 second. In order to further reduce the burning time, a considerably higher power must be applied.

On the other hand, an abnormal "flattening" of the curve at around 5 seconds can be observed. During this brief section between 11 and 13V, the burning time practically does not change. This could possibly be due to a lack of precision producing a significant variability of the measures. Calculating the burning time depends on factors such as the thickness of the thread, or its pressure against the resistance. Additionally, differences between resistances should be considered, as they are burnt and rendered useless after each measure, making necessary to change them every time. All this factors could explain this, although it is clear that the main trend is a decrease of burning time with increasing power, up to around 1 second.

Lastly, the energy consumption is also reduced while the voltage and power are increased. Although some unexpected peak is observed at 13 V, this may probably be caused by the measure uncertainty previously mentioned. Ideally, the higher the voltage the better. But, in reality, less voltage and a reasonable energy consumption value is recommended, as at higher values of voltage, the decrease of burning time could be considered negligible. For these reasons, the most suitable values should fall in the range of **10-15 V**, with burning times ranging from 2 to 10 seconds.

3.7.2 Circuit design

With the previous parameters defined, the circuit can be preliminary designed. The most suitable configuration would be a parallel circuit, as shown in Figure 3.23, in order to ensure that all the resistances get burned at the same time.

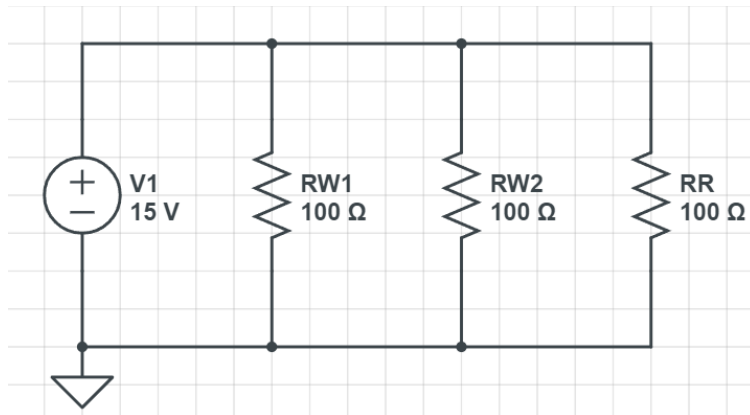


Figure 3.23: Preliminary circuit design (Source: Own elaboration)

As this is just a preliminary design, the complexity of this design could be improved through further development, for example, adding a relay in order to firstly burn the redundancy resistance that keeps the whole PocketQube stowed, and then burning the two remaining resistors at the same time, deploying the Solar Wings.

3.8 Simulation analysis

With the design defined, simulations are a great way of performing preliminary approaches to the behavior of the model during limit conditions, some of which will be finally tested in further sections. Due to the scope of the project, it has been decided to perform both **structural and modal analysis** to ensure the functionality of the design, as well as complementing this data with the lab testing.

The simulations have been done using ANSYS [40]. This software has been selected, among other things, due to its great performance in this type of simulations, as well as its availability and extensive documentation. Additionally, the setup and the results of the simulations will be based and contrasted by both the PocketQube standard [5] and the Falcon 9 User's Guide [41]. The SpaceX launcher has been selected by the availability of its documentation and its presence as one of the most prolific *smallsat* launcher in recent years.

Lastly, some considerations should be noted for this section. As stated in previous sections, the PocketQube model has been designed and prototyped using PLA, also known as polylactide plastic. The reason for this decision have already been mentioned, although it is mainly due to cost-effectiveness and availability of materials. However, PLA would not be the ideal material for a final, practical model that had to be launched into orbit. For this case, a feasibility study should be conducted on suitable materials for this purpose. Luckily, this has been the task of a final thesis by the HORUS mission, called *Study of commercially available FDM 3D printing polymers for their use on small satellites for the HORUS Project* [42].

As it is stated in the conclusions of this study, the selected materials for this type of design would be polyetherether ketone (PEEK) and polycarbonate (PC). Although PEEK has been more widely tested for this applications, PC is more suited to the scope and restraints of the HORUS project. For this reason, the simulations in this section will be performed using PC as the structure material instead of PLA.

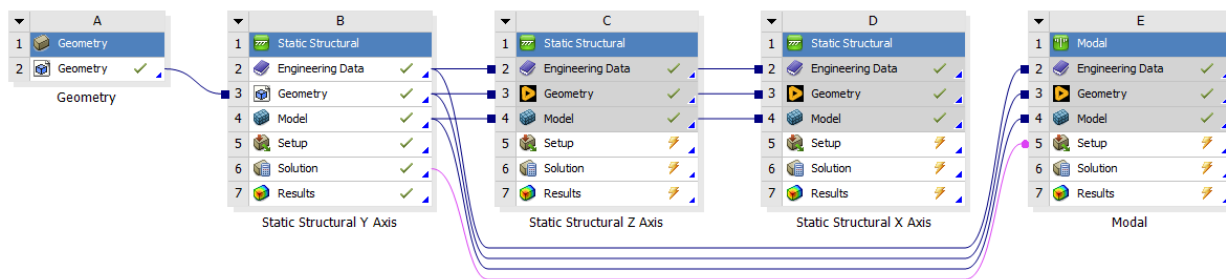


Figure 3.24: ANSYS Workbench simulations procedure (Source: Own elaboration)

3.8.1 Model preparation and meshing

In order to perform the simulations, it is first required to define the model and mesh, as well as introducing the right boundary conditions. Through ANSYS Mechanical, the CAD model designed in SolidWorks has been imported, with the coordinate systems defined in the PocketQube Standard [5]. The imported model is depicted Figure 3.25:

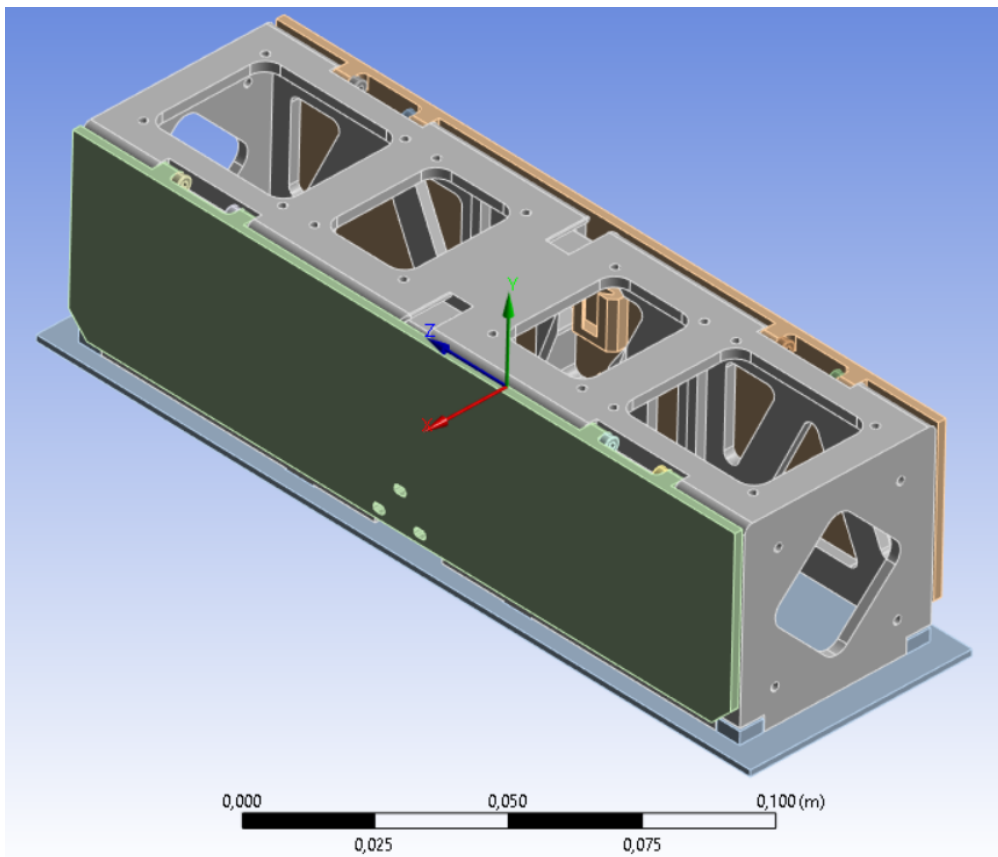


Figure 3.25: Model preparation in ANSYS, with its coordinate system (Source: Own elaboration)

Next, it is crucial to define both the mesh and the boundary conditions. Taking into account the satellite conditions during launch and deployment, as can be seen at Figure 2.2, a **fixed support** condition has been added to the laterals of the sliding backplate in order to simulate the effect of the deployer rail system. Additionally, it should be noted that the PocketQube has been simulated as a rigid body, neglecting the hinge boundary conditions, as it will be in a firm stowed position during launch.

Finally, a preliminary meshing has been performed on the model, with the final results shown in Figure 3.26. Additionally, the characteristics of the mesh are described in Table 3.5:

Table 3.5: Mesh parameters (Source: Own elaboration)

Mesh Parameters	
Nodes	121468
Elements	62720

It should be stressed that, although this mesh could be further optimized and refined for a more detailed simulation of the model, it serves just as a preliminary approach in order to validate the design for lab testing. For this reason, meshing optimization would, in this case, fall out of the scope of the project.

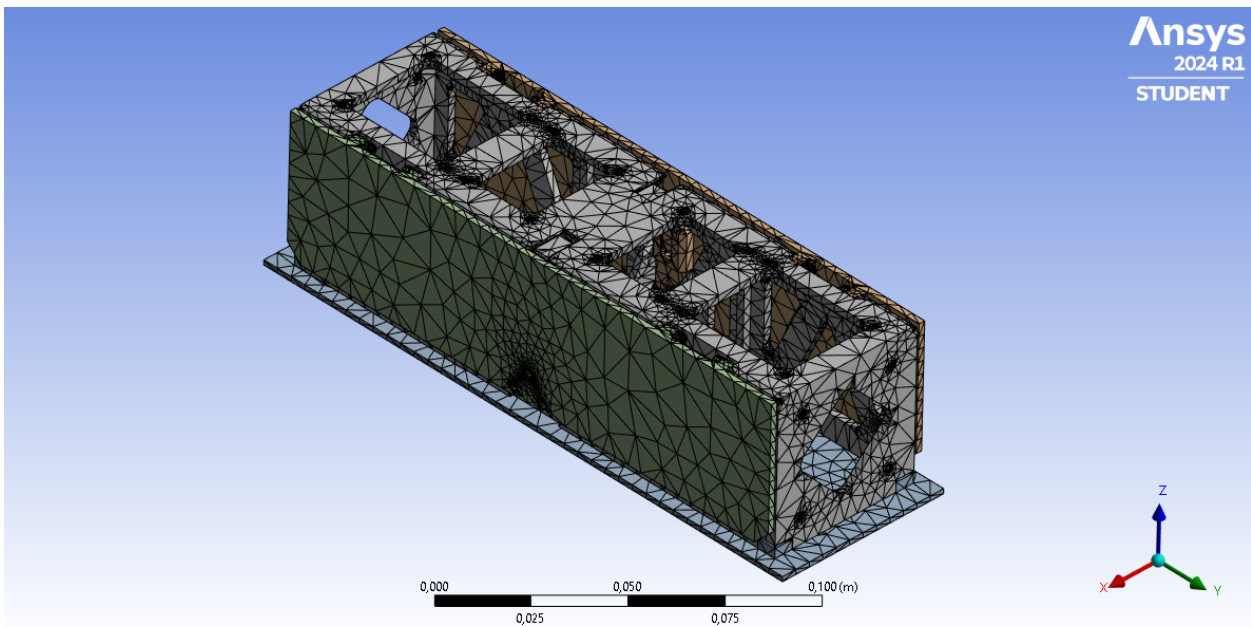


Figure 3.26: Model meshing (Source: Own elaboration)

3.8.2 Structural analysis

Once with the model properly defined, the structural simulation has to prove that this design has the capability of withstanding the launch accelerations environment. For this purpose, the Falcon 9 flight load limits, extracted from the launcher's user guide [41], are presented below in Figure 3.27:

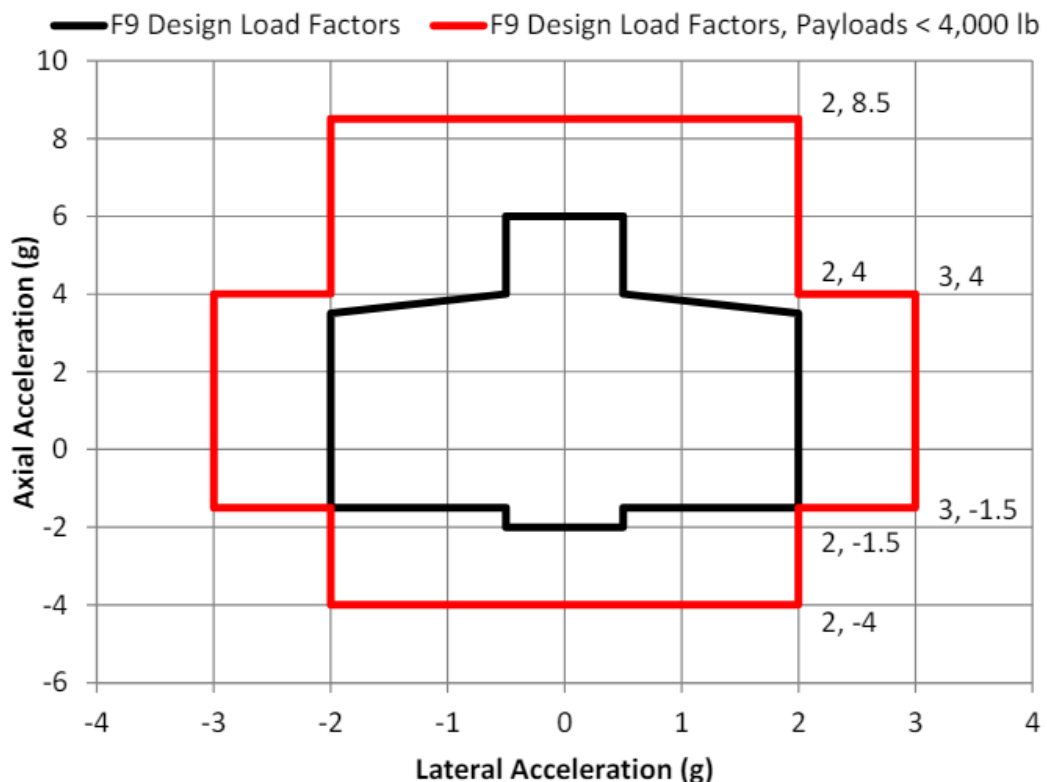


Figure 3.27: Falcon 9 flight load limits (Source: [41])

As can be seen, for payloads below 4000 lb (around 1800 kg), the load limit is defined by a maximum axial acceleration of 8.5 g and a top lateral acceleration of 3 g in certain regions. However, as the orientation of the satellite in the deployer respect the launcher coordinates is, at the time, undetermined, the maximum acceleration will be applied individually to each axis of the PocketQube. This way, the worst case scenario will be taken into account, with a reasonable safety factor. The simulation results are summarized in Table 3.6:

Table 3.6: ANSYS Structural Analysis Results (Source: Own elaboration)

PC		Steel		
	Max Stress (Pa)	SF	Max Stress (Pa)	SF
Y Axis	8,49E+04	729,46	6,87E+05	364,17
Z Axis	8,63E+04	717,38	8,11E+05	308,33
X Axis	5,14E+05	120,52	8,39E+06	29,79

It should be noted that the results represent the **Equivalent Von Misses Stress**, and that the safety factor coefficients have been calculated taking into account the **tensile yield strength** of each material, extracted from ANSYS [40] Engineering Data, which is shown in Table 3.7:

Table 3.7: Materials tensile yield strength (Source: Own elaboration)

Tensile Yielding Strength (Pa)	
PC	6,19E+07
Steel	2,50E+08

As can be observed, the simulation results have been divided into materials and axis. In all cases, the SF values are more than enough to validate the design. However, there are some interesting conclusions that can be drawn from these results.

Firstly, it can be observed that the steel components, the screws, are subjected to a significantly higher stress (around one order of magnitude higher) than the rest of the assembly. In fact, the hinge assembly, even stowed, is where the highest stress are concentrated, for both PC and steel components. Figures 3.28 represent the simulation results in the hinge regions for both PC and steel components:

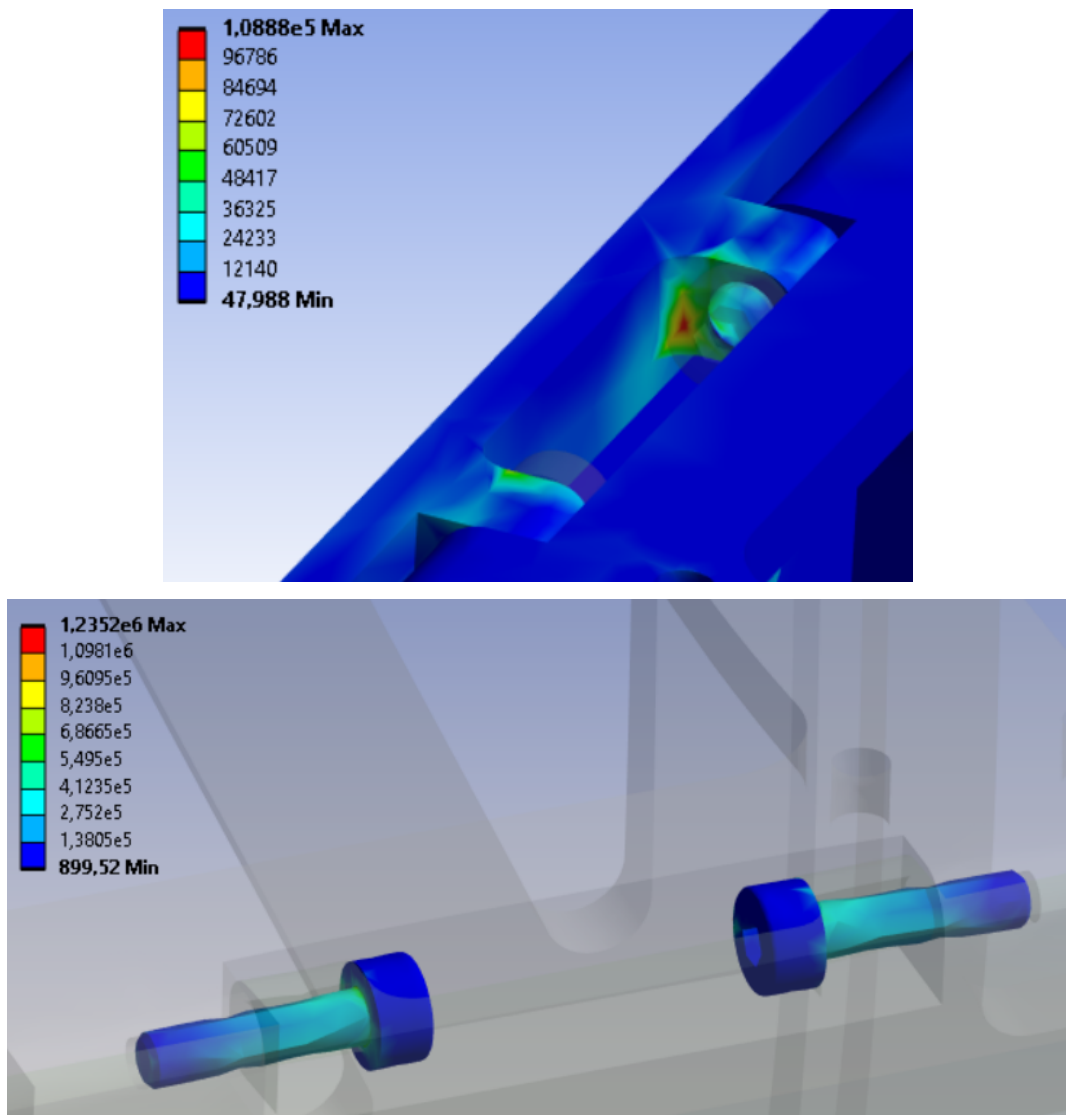


Figure 3.28: Stress at the hinge region (Y Axis acceleration) (Source: Own elaboration)

Although the design will be able to withstand the worst launch loads with ease, it is important to remark that the hinge system is the most critical part of the design in this matter. As possible further development, an in-depth and more detailed study could be made in this area in order to reduce its criticality.

Returning to the simulation results, it is interesting to note the difference between the different axis. As expected, the X axis is the weakest orientation of the PocketQube, with maximum stresses being between five to ten times higher in this position. However, as deployers usually eject the payload radially to the launcher axis, the most plausible configuration would be one with the Y axis sustaining the biggest flight loads (axial forces). Figures 3.29 represent the distribution of stress in all three simulations:

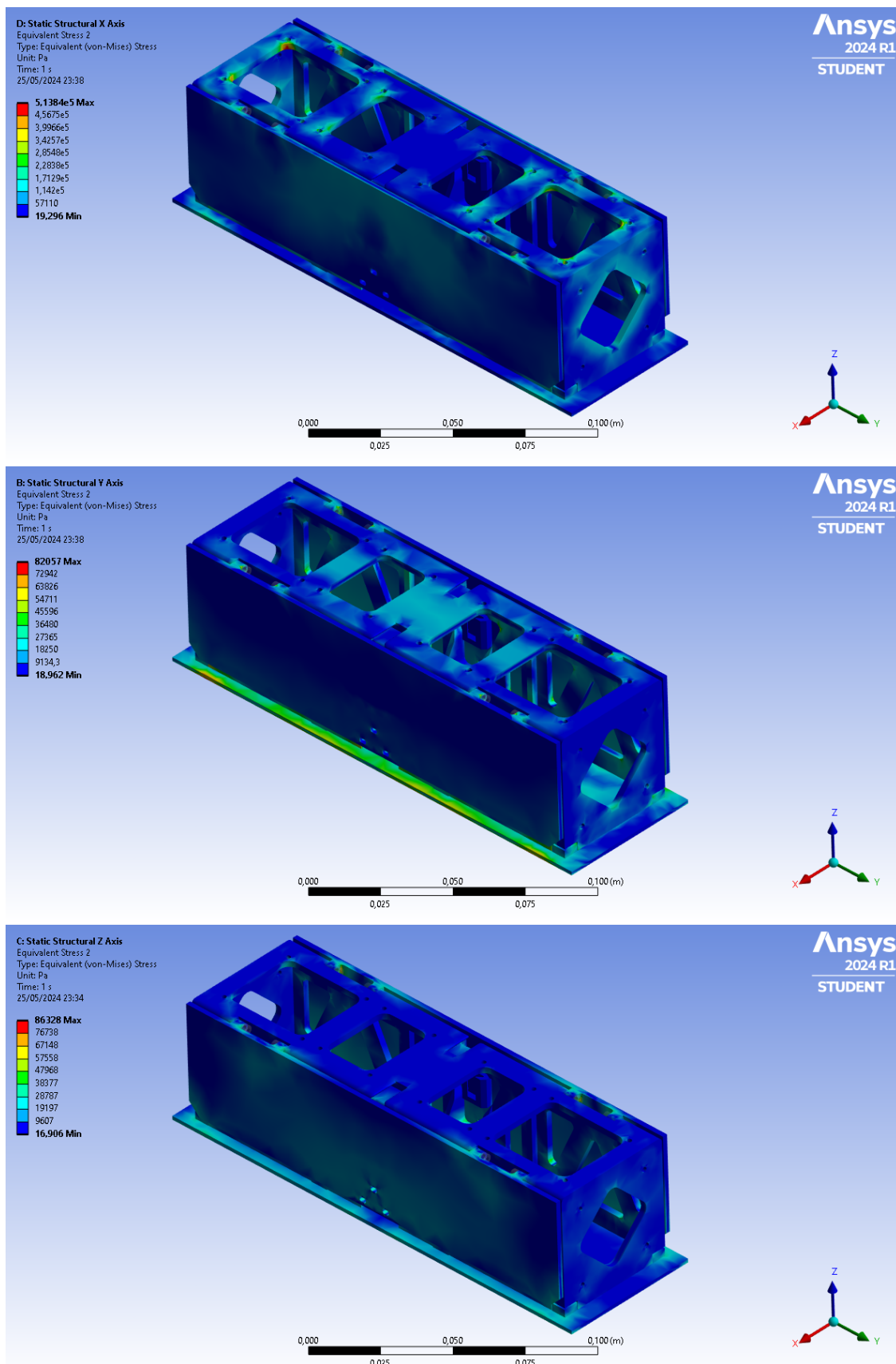


Figure 3.29: Stress distribution with loads on the X axis (above), Y axis (center) and Z axis (below) (Source: Own elaboration)

In conclusion, the structural simulations results are considered satisfactory, and prove that the design is capable of withstanding, with a considerable margin of error, the launcher's flight load.

3.8.3 Modal analysis

With the results of the structural analysis, the next simulation step, and possibly the most crucial one, is the modal analysis. The analysis of the natural frequencies of the PocketQube is key to understand its behavior under the vibration environment of launch. The resonance frequencies, as well as its amplitude and effect on the structure, will determine the capabilities of the model to survive the launch, as resonance phenomenon can be really destructive and dangerous for the mission.

In order to characterize the simulation environment, the vibration data has been obtained from the Falcon User's Guide [41], as well as the SMC-S-016 [43], the Air & Space Force standard titled *Test Requirements for Launch, Upper-Stage and Space Vehicles*, with the PSD depicted in Figure 3.30.

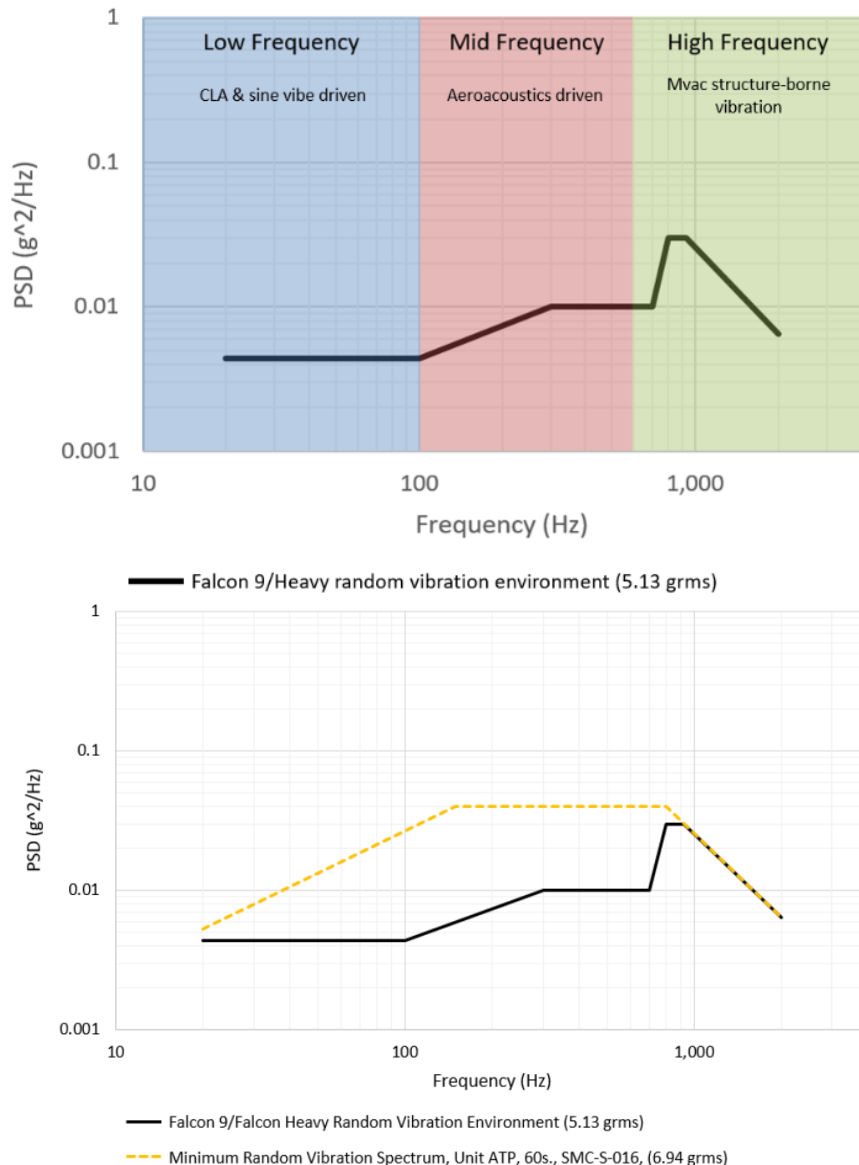


Figure 3.30: Falcon 9 and Heavy frequency bin (Source: [41])

As can be extracted from the pictures above, the frequency range for the modal analysis should include frequencies up to 2000 Hz in order to study all existent modes during launch. Concretely, in order to consider the worst case scenario, the SMC-S-016 frequency distribution will be used. Although higher than the expected Falcon launch conditions, this situation would prove that the model complies with the regulations to fly in any other launcher. The results of the modal analysis are presented below in Figures 3.31 and 3.32:

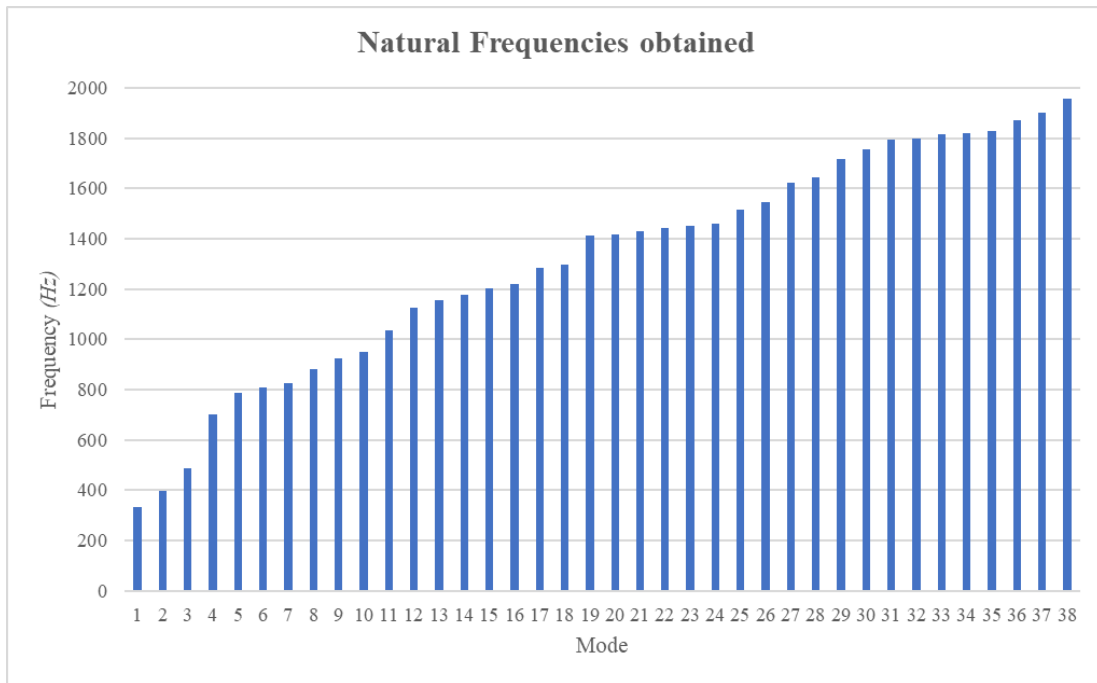


Figure 3.31: Natural frequencies obtained in the modal analysis (Source: Own elaboration)

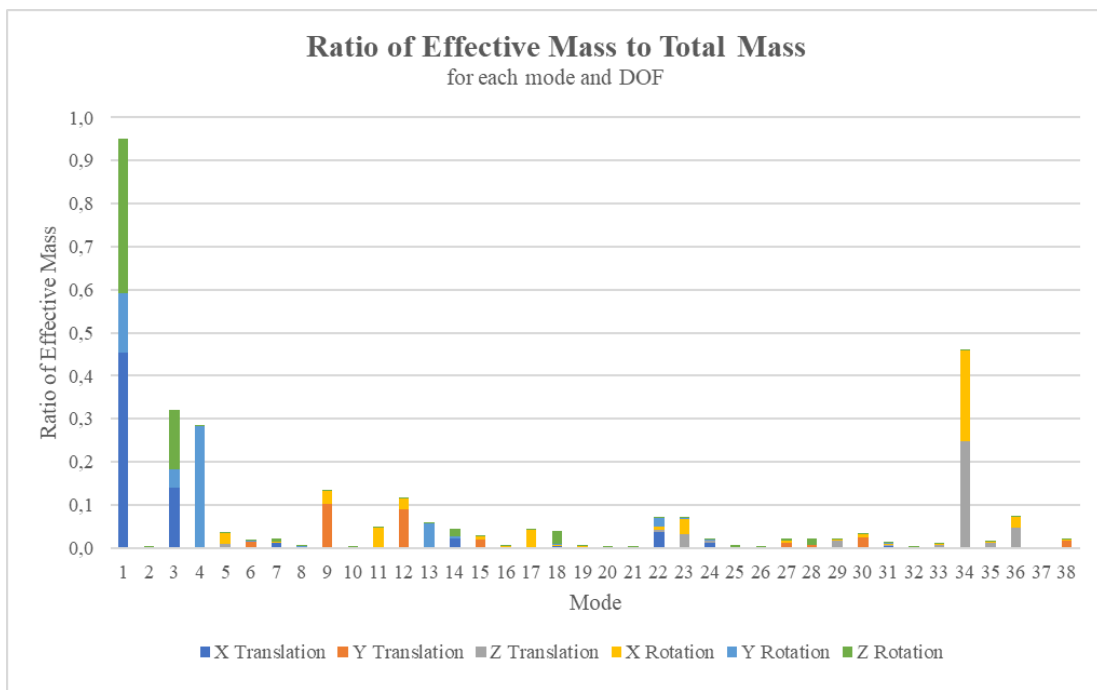


Figure 3.32: Effective mass ratio for each mode and ratio (Source: Own elaboration)

As can be observed, the main modes of the structure in the designated frequency range are Modes 1, 3, 4, 9 and 34, with Modes 12, 13 being sub modes. The rest of modes can be ignored as their mass fraction is negligible. However, it can be observed that the mass fraction summation does not represent the totality of modes, which means that, quite probably, some main modes are not represented, as they will appear at higher frequencies (more than 2000 Hz). Additionally, it should be noted that the coordinate system used in the table is based on the PocketQube Standard coordinates depicted in Figure 3.25.

Now, it would be interesting to individually study each main and sub mode in order to determine its effect on the model behavior:

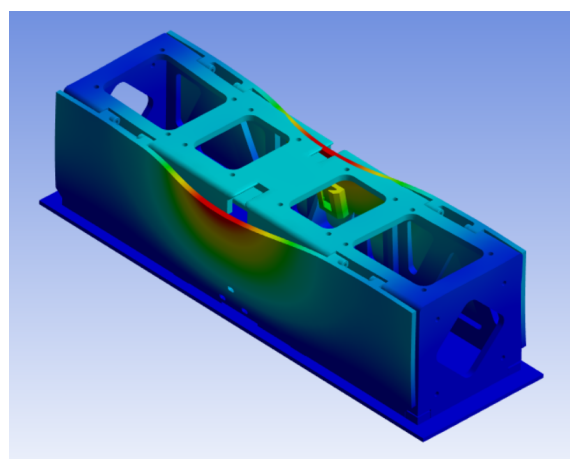
Main modes

- **Mode 1:** This mode is the principal mode for X translation and Z rotation, although it also has a main contribution in the Y axis rotation. At 331 Hz, this also represents the first mode to appear upon vibration, so it should be considered as the main concern during launch conditions. As can be seen in 3.33, it mainly affects the Solar Wings.
- **Mode 3:** This main mode has moderate contributions in X translation and Z rotation. It is similar to Mode 1.
- **Mode 4:** This mode represents the principal contribution in the Y rotation axis. It is also located at the Solar Wings.
- **Mode 9:** This resonance mainly affects the sliding backplate, being the principal and only main mode for Y translation.
- **Mode 34:** This mode appears at a high frequency, at 1822 Hz, and represents the only main mode in Z and X rotation. It is a very complex resonance that significantly affects the complete model.

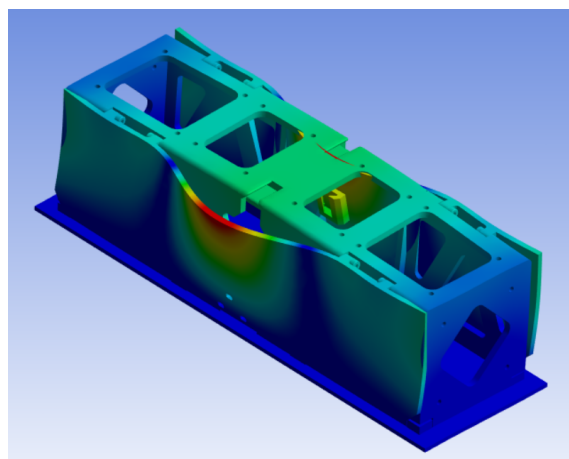
Sub modes

- **Mode 12:** With a dominant contribution in the Y translation axis, this mode primarily affects the Solar Wings and the main box.
- **Mode 13:** This mode mainly resonates in the Y rotation axis. Moreover, as the last sub mode, it is produced on the Solar Wings and the main box.

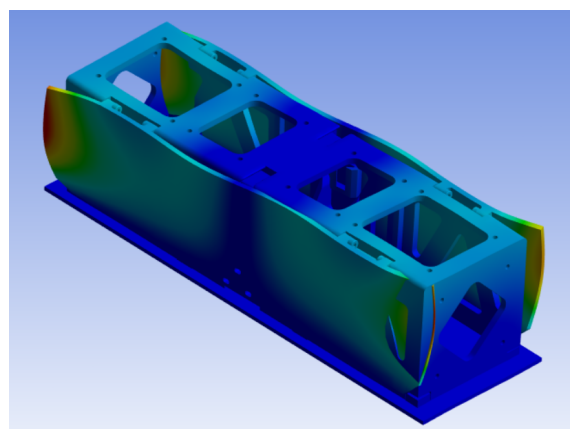
Next, the representation of the modes in ANSYS is provided in Figures 3.33 and 3.34 for clarity:



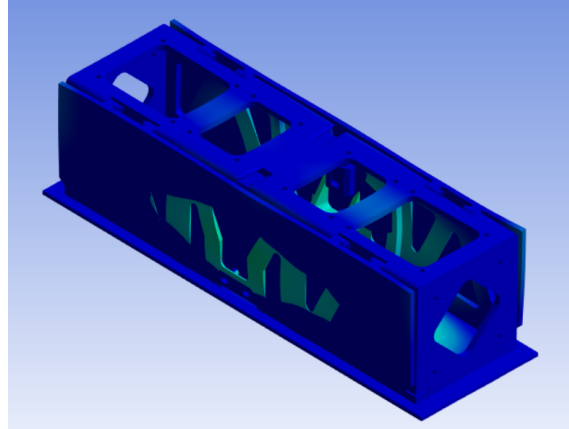
(a) Mode 1



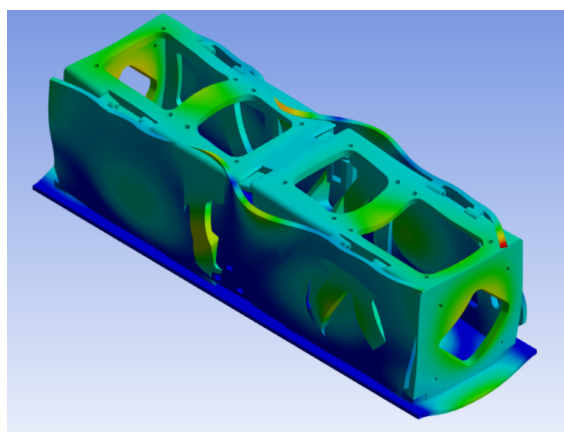
(b) Mode 3



(c) Mode 4

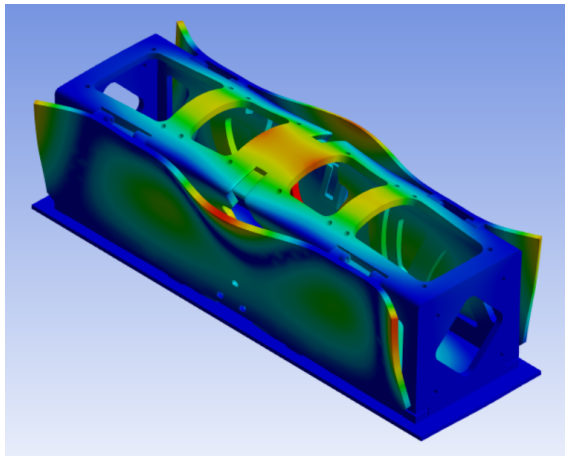


(d) Mode 9

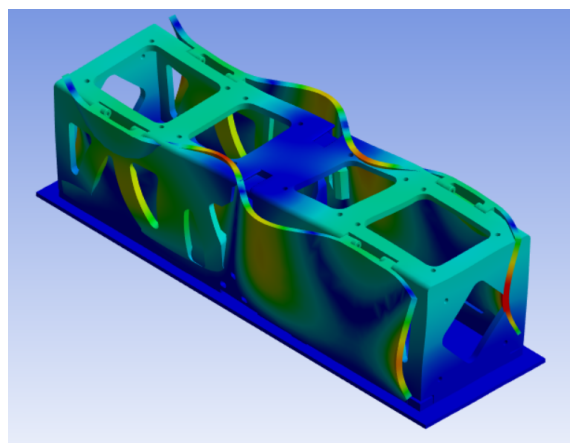


(e) Mode 34

Figure 3.33: Main modes deformation (Source: Own elaboration)



(a) Mode 13



(b) Mode 13

Figure 3.34: Sub modes deformation (Source: Own elaboration)

The results of the modal analysis provide interesting information about the model. As expected, the Solar Wings are the main source of resonance, as well as the component most affected by them. The modes vary in complexity and form in all the DOFs of the model. Through the launch conditions, 38 modes have been calculated, although only the 7 mentioned should be considered.

Finally, in order to assess the impact of the modal analysis for the launch behavior and compliance of the design, the Mission Success Handbook for Cubesat Missions [44] from NASA Standards has been used, due to a lack of similar requirements in the PocketQube standard. According to this document, only satellites with modes under 100 Hz should perform additional tests to verify the design suitability. Which means, that, in the case of this project, the design can be considered compliant, as the first mode appears at 331 Hz.

3.9 Testing

Once the 3P PocketQube is fully designed, testing is the next step in order to validate its performance during the mission. The most critical part of it is the launch environment, where the design is subjected to the greater loads and perturbations. Additionally, in order to embark a mission in any launcher, it has to previously comply with regulations in order to confirm that it can withstand the flight conditions. In the case of this project, the model will be subjected to random vibration testing [45]. This type of test differs from the sinusoidal vibration test, as it excites the model with a random signal based on a given frequential spectrum. This type of tests allow to observe the behaviour of models during realistic perturbations, and typically are used to bring the model to failure.

As discussed in Section 3.8.3, the random vibration environment during launch is provided for the launcher's user guide [41], as well as from the Air & Space Force [43]. The latter will be taken into account, as it is the most restrictive environment. The PSD is provided below in Figure 3.35:

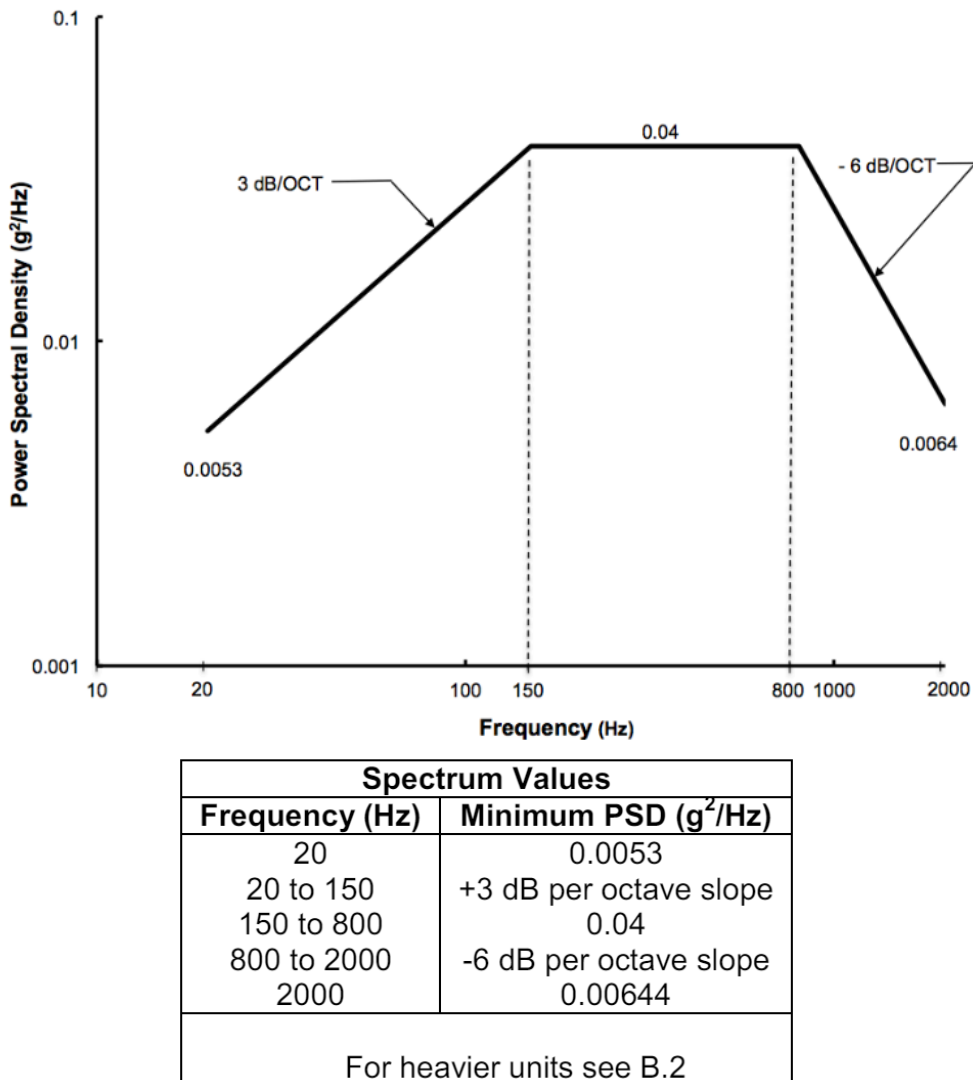


Figure 3.35: SMC-S-016 minimum random vibration environment during launch (Source: [43])

The testing will be performed in the university facilities, more specifically at the **Acoustical and Mechanical Engineering Laboratory** (LEAM) in UPC Terrassa. In order to perform the test, a shaker configuration with axial vibration shall be used. The model will be placed in its stowed position and a determined random vibration signal will excite the shaker for at least 160 seconds, which is the approximate duration of a Falcon 9 launch until MECO (Main Engine Cut-Off) and stage separation [41].

For that purpose, a random vibration signal with the provided PSD in Figure 3.35 must be created. This will be done using Matlab. Firstly, the input parameters are defined, with a sampling frequency of 4096 Hz, as the maximum frequency of the PSD is 2000 Hz. After the PSD slopes are defined and the random signal generated accordingly, a PSD can be generated from the random signal in order to compared to the one provided by regulations. Using `pwelch` and a Hamming window, it can be observed in Figure 3.36 that the generated signal fits perfectly the desired curve.

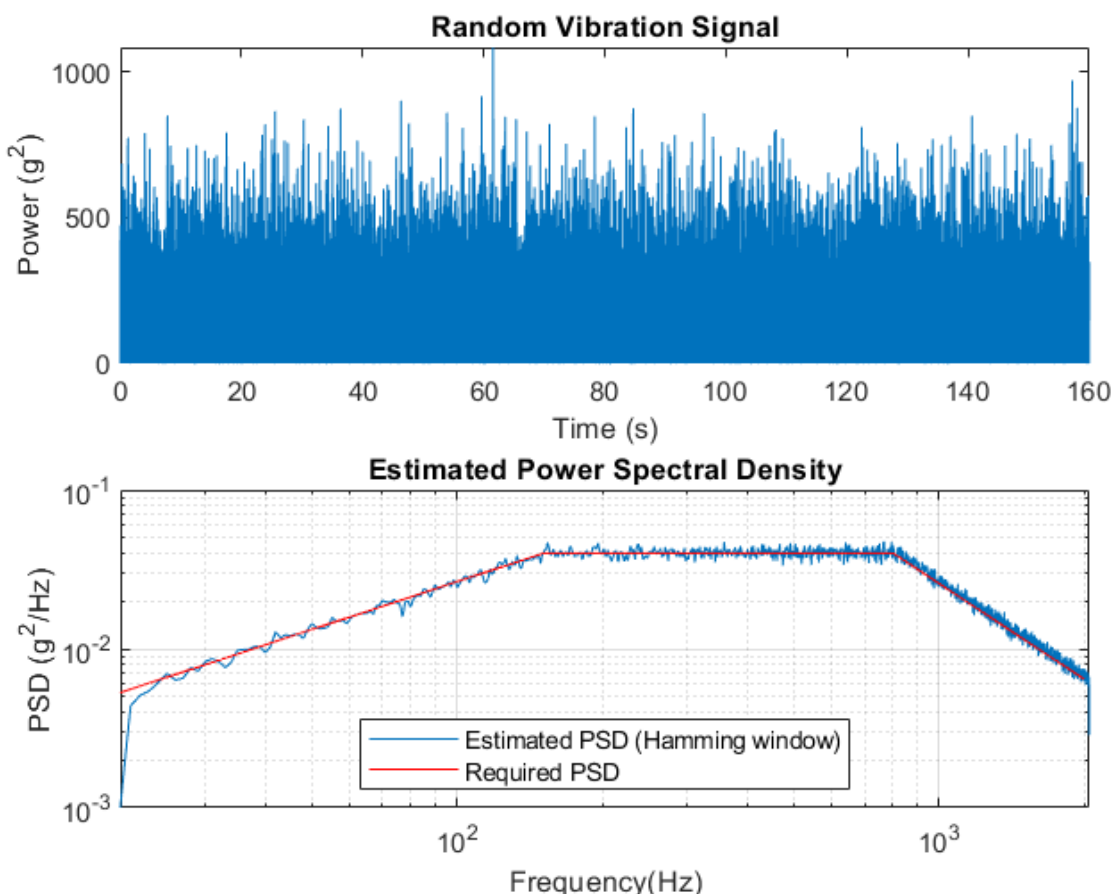


Figure 3.36: Random generated signal and its PSD, compared to the required PSD (Source: Own elaboration)

The code created in order to generate the random signal is provided below in Listing 3.9:

```

1 clear; close all
2
3 %% Input parameters
4 Fs = 4096; % Sampling frequency (Hz)
5 T = 160; % Signal duration (s)

```

```

6 N = T * Fs; % Number of samples
7
8 %% PSD
9 f = [20, 150, 800, 2000]; % PSD frequencies (Hz)
10 psd_values = [0.0053, 0.04, 0.00644]; % PSD values (g^2/Hz)
11
12 Pxx = zeros(N/2+1,1); % PSD Initialization
13 freq = linspace(0, f(4), N/2+1); % Frequencies
14
15 % Values assignation
16 Pxx(freq >= 20 & freq < 150) = psd_values(1) * (freq(freq >= 20 & freq < 150) / 20);
17 Pxx(freq >= 150 & freq <= 800) = psd_values(2);
18 Pxx(freq > 800 & freq <= 2000) = psd_values(3) * (2000 ./ freq(freq > 800 & freq <= 2000))
    .^2;
19
20 %% Random signal
21 Sxx = sqrt((N/2+1)*Pxx .* (Fs/2));
22 Sxx = [Sxx; flipud(Sxx(2:end-1))];
23 Sxx = Sxx .* (randn(N, 1) + 1i * randn(N, 1)); % Complex White noise
24
25 %% Inverse fourier transform
26 signal = ifft(Sxx, 'symmetric');
27 signal = signal(1:N); % Normalisation
28
29 power_signal = signal.^2; % Obtain power (g^2)
30
31 %% Plotting
32 figure;
33 % Random signal
34 subplot(2,1,1);
35 plot((0:N-1)/Fs, power_signal);
36 xlabel('Time (s)'); ylabel('Power (g^2)');
37 title('Random Vibration Signal');
38
39 % PSD
40 subplot(2,1,2);
41 [Pxx_est, f_est] = pwelch(signal, hamming(4000), [], [], Fs);
42 loglog(f_est, Pxx_est);
43 hold on
44 loglog(freq,Pxx,'r')
45 xlabel('Frequency (Hz)'); ylabel('PSD (g^2/Hz)');
46 xlim([f(1),2048]), grid on
47 title('Estimated Power Spectral Density');
48
49 legend('Estimated PSD (Hamming window)', 'Required PSD', 'Location', 'south')
50 save('power_signal.mat', 'power_signal')
51 audiowrite("power_signal.wav", signal, Fs)

```

Listing 3.1: Signal generation code (Source: Own elaboration)

As can be observed, the signal is finally saved in a .wav file, in order to be able to reproduce it in the shaker. Then, the setup can be finally mounted with the shaker, the generated vibration signal loaded and the model placed on top of the shaker. The shaker used for this test is a **Brüel & Kjær Type 4825** [46]. It should be noted that the model has been fixed to the shaker with bee wax, and that an accelerometer has been fixated to the center of the sliding backplate, where the model is in contact with the shaker. The test mounting is depicted below in Figure 3.37:

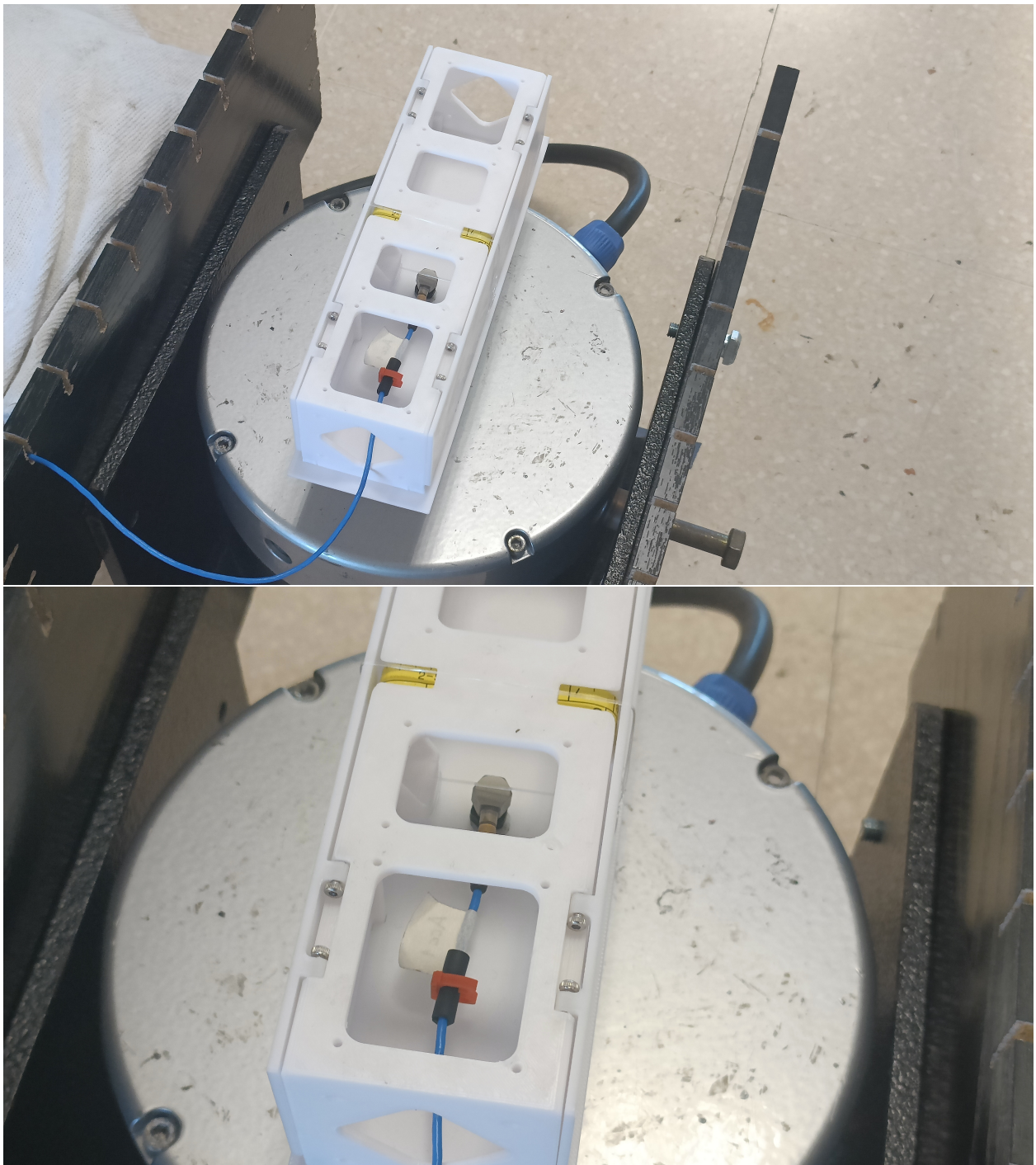


Figure 3.37: Image of the test setup, with the shaker, the model, and the accelerometer on the sliding backplate (Source: Own elaboration)

With the test setup mounted and ready, the testing can begin. The generated random vibration is transmitted through the shaker to the model for 160 seconds. The accelerometer reads the vibration on the model next to the shaker in order to validate that the design is exposed to the correct signal vibration, and then performs a PSD of the signal. If this PSD is compared with the required fequential spectrum of SMC-S-016, the graph depicted in Figure 3.38 is obtained:

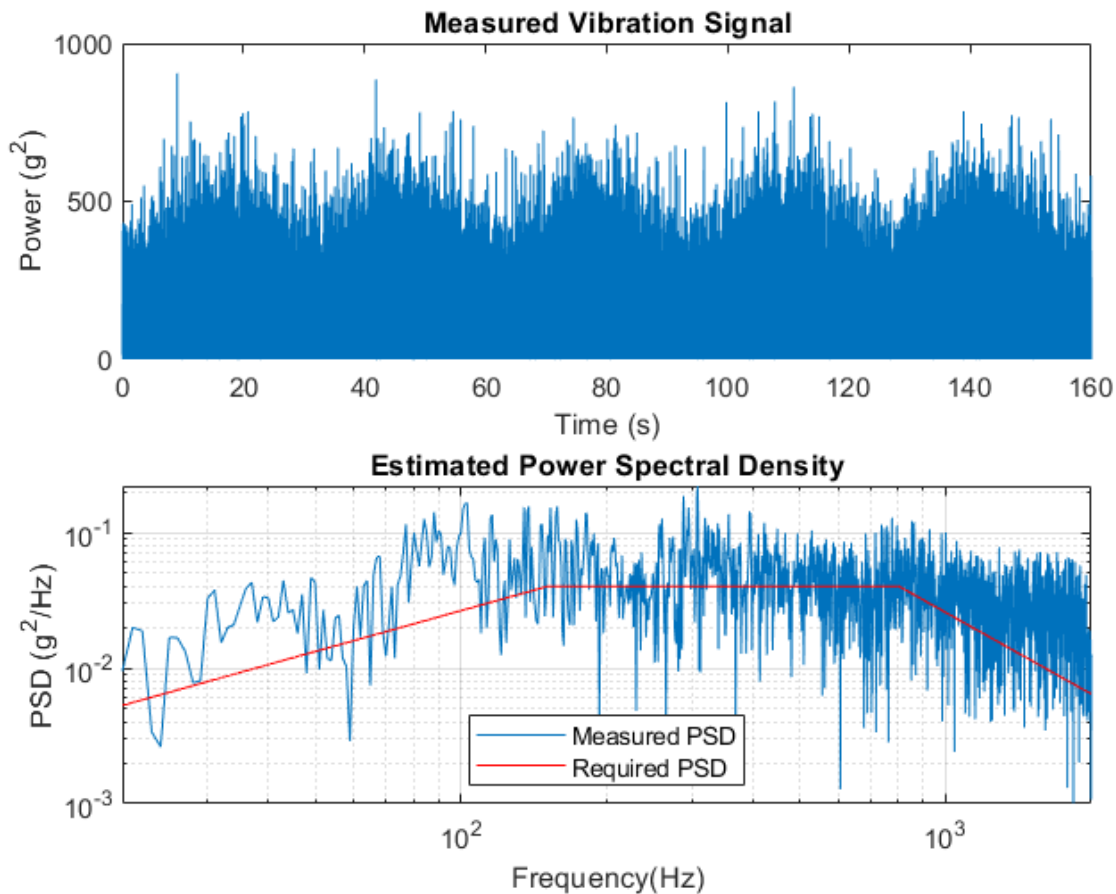


Figure 3.38: Measured signal and its PSD, compared to the required PSD (Source: Own elaboration)

As can be seen, the PSD correctly matches the required one specified in the SMC-S-016 regulation. The observed perturbations of the signal are expected due to the characteristics of the shaker, external vibrations and the fact that the accelerometer is not exactly placed on the shaker itself, but on the sliding backplate above it. However, the fitting of the results can be considered satisfactory.

And, what is most important, the qualitative assessment of the PocketQube after the test was successful. The design maintained its integrity in its stowed position. The bolts remained fixated, and the HDRM mechanism was tight and resisted the vibration. In conclusion, the test can be considered a success, and proves that the model complies with launch regulations.

3.10 Scalability to other configurations

While the 3P model has been considered the main and most critical design, PocketQubes allow for a wide range of configurations, as happen with CubeSats. As discussed in Section 2.2, deployable panels are typically used in PocketQubes from 2P to 3P configurations, where the increased payload volume makes necessary for additional power. For this reason, a feasibility study will be performed, with emphasis on the concept of a 2P and 2.5P PocketQube with deployable panels.

The main limitation as the frame gets smaller is the surface availability to fit the solar panels. Due to the standard measures of COTS solar cells, the typically provided size for this component is 4x8 cm. However, Azurspace [22] also provides a 4x7 cm solar cells with the same characteristics that the selected cell for the 3P model. This component could be used in a 2.5P configuration, as this solar cells allow for more surface efficiency and, thus a higher power to volume ratio. Finally, the 2P configuration is so small that only one solar cell can be fitted into each Solar Wing, significantly reducing both the used surface and power ratio. The summary of the feasibility study can be observed in Table 3.9:

Table 3.9: Scalability feasibility study (Source: Own elaboration)

	1P	1.5P	2P	2.5P	3P
Power (W)	-	3,31	3,31	5,82	6,63
Used Surface (%)	-	82,15%	59,09%	81,06%	75,69%
Power/Volume (W/m³)	-	23,29	15,44	20,31	18,48

As can be seen, although the 3P configuration generates more power with the current design, a 2.5P configuration would be the most efficient and optimized one, taking into account the selected Solar Cells components. It should also be stressed that, although an assessment for 1P and 1.5P configuration has been performed, the need for deployable solar panels in PocketQubes only appears for larger configurations (as mentioned in previous sections), as this is where the power limitations start to become noticeable. As can be observed in the previous, table, the 1.5P configuration has the highest optimization, although this design is incompatible with the actual HDRM systems, and minor changes should be implemented in the design. Additionally, there are no COTS solar cells provided by Azurspace that can be fitted on a 1P PocketQube. And, in any case, the complexity of the deployment mechanism starts to outweigh its advantages as the configuration gets smaller. This, added to a lack of interest in deployable system at smaller configurations, makes unlikely to fully develop a working model with these specifications.

In conclusion, the scalability study makes clear two important points. Firstly, the characteristics and availability of the solar cells are key to defining the performance of the designs and its feasibility. And lastly, with the current selected components, the **2.5P** and **3P** configurations stand out as the best options for the design, as the increased power advantages are paired with the added complexity of a deployment system. On the other hand, a 2P configuration has a low efficiency, and from this point, the rest of configurations start to present incompatibilities with the actual design that makes them less desirable.

Next, some images and comparisons between all the configurations (1P, 1.5P, 2P, 2.5P and 3P) are depicted in Figures 3.39 and 3.40. The blueprints of all the designed configurations are available in the Blueprints Annex.

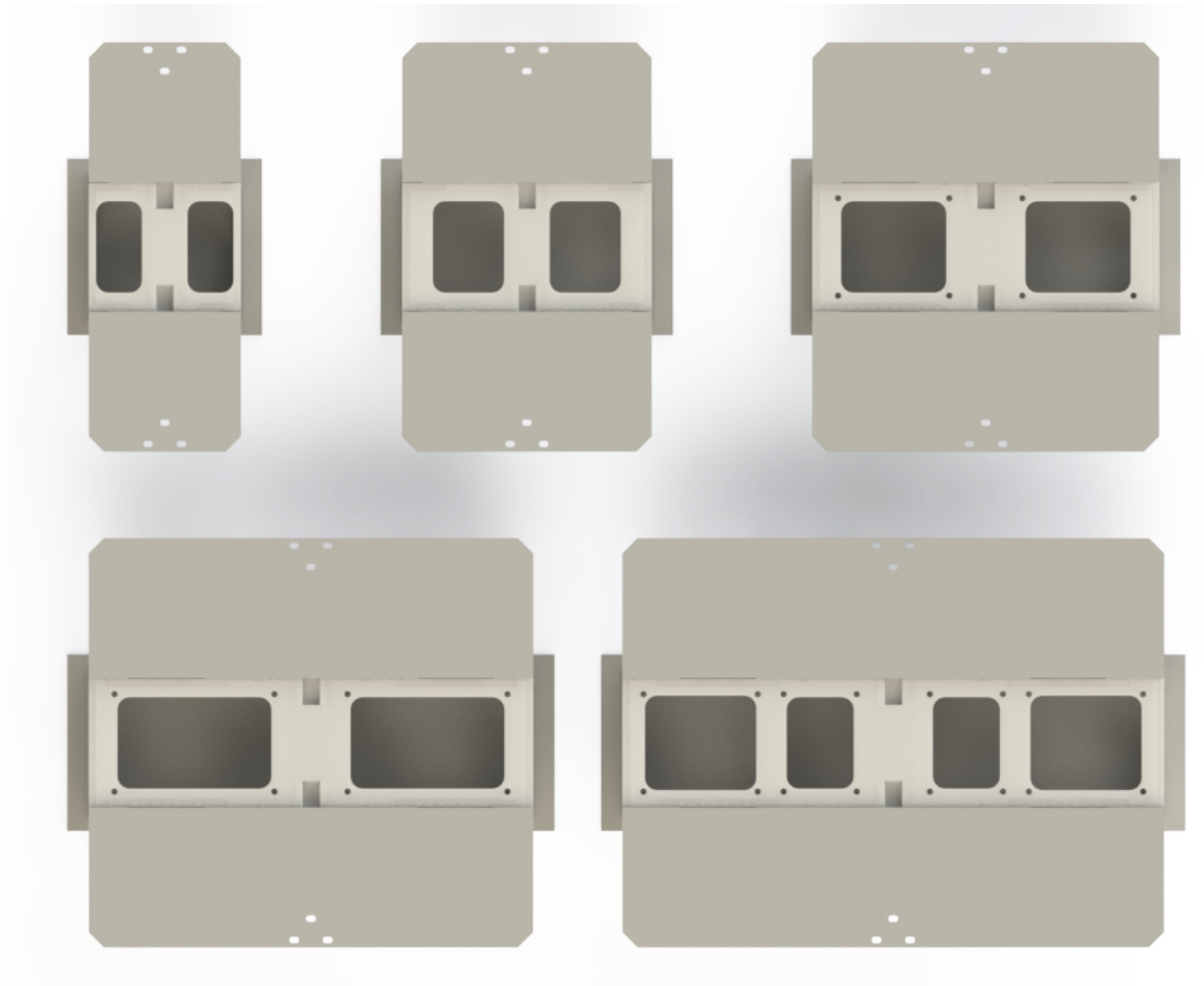


Figure 3.39: Top view of different configurations (Source: Own elaboration)

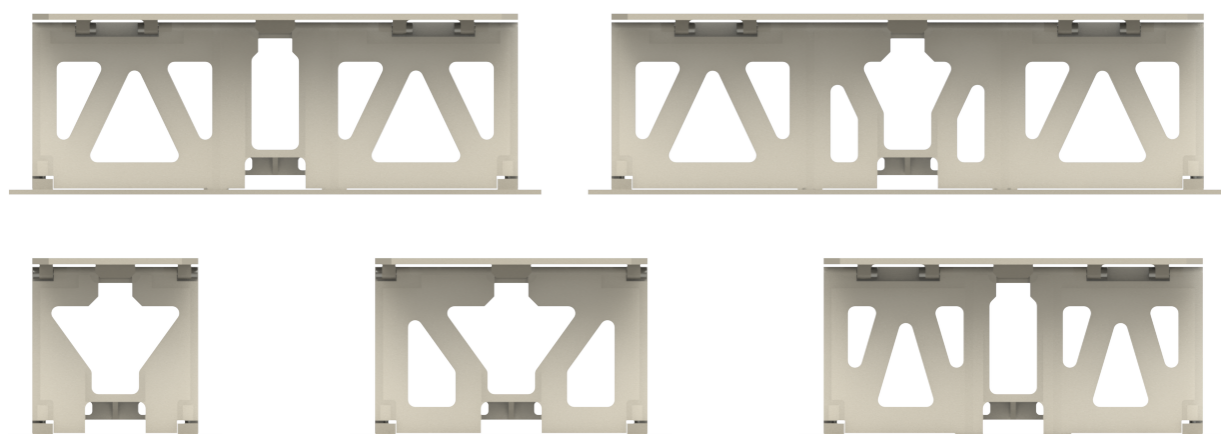


Figure 3.40: Side view of different configurations (Source: Own elaboration)

Chapter 4

Budget summary

As the scope of the project includes both the design and building of the model, both technical and execution costs are represented. The budget has been divided into several key categories to ensure comprehensive coverage of all expenses. Each category encompasses specific items and activities required to successfully complete the project.

For example, Design and Prototyping costs include engineering fees, software licenses, and materials for creating prototypes. Building costs cover the materials, components, and labor required for the construction of the picosatellite. Testing costs account for the necessary tests and lab infrastructure to ensure the satellite meets industry standards and performs reliably.

The total budget summary shown in Table 4.1 provides an aggregated view of the financial requirements, ensuring that all aspects of the project are adequately funded. The summary is presented below, although a detailed breakdown is provided in the Budget Annex.

Table 4.1: Budget Summary (Source: Own elaboration)

Concept	Cost
Design	14.785,00 €
Prototyping	810,00 €
Assembly	406,92 €
Testing	700,00 €
TOTAL	16.701,92 €

Chapter 5

Analysis and assessment of environmental and social implications

The picosatellite sector, as part of the New Space, has brought important environmental and social changes to the space industry. Firstly, the development of smaller satellites has reduced both complexity and cost of the missions, allowing for a wider range of users to define and launch their payloads. This has been especially noticeable in the academic institutions, where *smallsats* have allowed the students and research groups to develop their missions and experiments.

With this project, the goal is to further increase availability of these technologies, by reducing costs and complexity. By providing an already designed, proven system that is certified for space missions, this PocketQube kit can be easily adapted to any experiment that can fit in its payload bay. The use of COTS components, as well as everyday materials and 3D printed structures, makes possible for almost everyone to build the kit on their own. Moreover, the aim of this kit, when all of its subsystems are designed and certified, is to be released as an open source platform for everyone to use. And, building upon the New Space trend, increased access to space has its numerous and tangible social and environmental effects [47].

For example, a wider and easier access to space allow for more space technologies to be developed and tested in these environments, further fostering the research of important technologies that range through all the areas in our lives: from medicine to automotive industry, the research of these technologies has proven again and again to have a positive and tangible effect in everyday life [48]. However, besides the undeniable research improvement, globalisation of space access also has a positive effect in education, for example. Allowing engineering students to develop space missions is a great way to put their knowledge into a practical project that will have real-world applications. Additionally, the multidisciplinary character of these systems makes them a great chance to boost cooperation between groups, and even between other specializations.

On the other hand, the environmental implication of the project must be discussed. While the massive access to space will undoubtedly result in a greater number of objects in orbit, the low orbits of these missions are translated into shorter life spans. Where older and bigger satellites had a life of 20+ years, the modern smallsats do not usually last more than 5 years. Additionally, the lower orbits (as seen in Figure 5.1) and increased drag are responsible for a quick de-orbitation of the space debris, where bigger satellites placed into higher orbits are placed into crowded graveyard orbits, or simply abandoned. In a sector where space debris is one of the biggest concerns [49] [50], this type of missions have emerged as a way to avoid overcrowding our lower orbit.

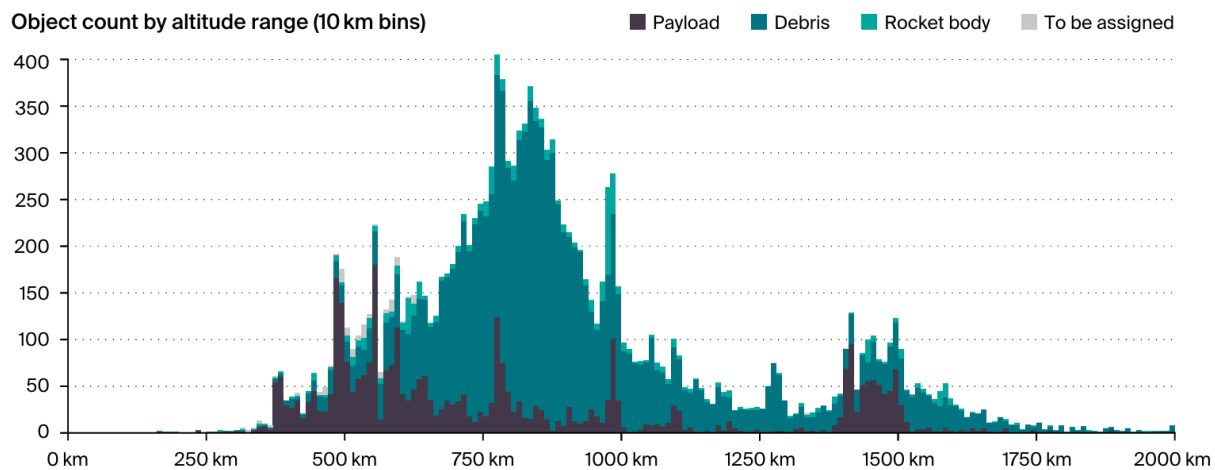


Figure 5.1: Representation of LEO population of satellites and debris. Most smallsats missions are orbiting in 350-700 km orbits, resulting in a rapid and safe de-orbiting after their mission lifespan (Source: [51][52])

Finally, the use of COTS components and accessible materials [53] does not simply make the kit more accessible and reduce building costs. It also promotes sustainability by encouraging the use of recyclable and reusable materials, reducing the overall environmental footprint of satellite production. Additionally, the potential for customized 3D printing components minimizes waste and allows for the use of eco-friendly materials. These sustainable practices are not only in line with global environmental goals but also set a precedent for future innovations in the space industry to prioritize eco-conscious design and manufacturing.

In conclusion, the project does not simply align with the actual trends of the space sector, but allows for new and more accessible projects in our closest environments.

Chapter 6

Conclusions

As stated in the introduction, the main objective of this project was to design, build and test a solar panel deployment system for PocketQubes. After all the work shown in this report, a design model for a 3P PocketQube has been designed and built, proving his deployment capability and performance. This model has been subjected to modal and structural analysis in order to comply with the critical launch environment. And, finally, the design has been tested with the random vibration environment imposed by regulations, proving to be capable of sustaining the flight conditions.

Additionally, this 3P model and its deployment system has been escalated to 1P, 1.5P, 2P and 2.5P configurations. Although the feasibility of these designs are dependant by the availability of COTS solar cells alternatives, the system itself and its performance is satisfactory. The best performing models, in solar power terms, are, with the selected components, the 2.5P and 3P configurations.

This project has proven the capability of building a cost-effective, simple deployment system with COTS components and 3D printed materials, successfully achieving the goals of the HORUS mission and bringing space access closer to the general public. However, it is important to highlight that the greatest limitation of the design is the availability of COTS components, especially with solar cells. As the alternatives are sometimes limited or imposed, the design must be altered to solve these requirements. However, the overall result can be considered satisfactory.

6.1 Further development

In any case, this project, due to its complexity, still has a great margin for improvement and further study. For example, an extensive test campaign could be performed to the design, not only in all its different configurations, but also in all the launch and missions conditions, which involve shock, thermal and acceleration tests, among others. Only with a complete and thoughtful testing, the design will be fully certified for space.

Simulations could also be performed with optimized meshing, and focusing on the most critical part of the assembly, the hinge. The results could help to improve the design, reducing stress, loads or resonant

frequencies. Other areas of the design could be improved through this concept, such as the topological design, reducing weight and volume while maintained strength.

Secondly, a development of the preliminary electric circuit of the HDRM subsystem is also highly recommended. The simplicity of the actual design has great room of improvement, with the addition, for example, of relays and board controllers in order to make the deployment smoother, as well as improving telemetry and control during the mission.

Moreover, other design concepts could be studied, such as the nichrome burning wire or the shape metal alloy mechanisms. The reducing costs of these technologies could make them feasible in the short term, and a design concept with this characteristic would be interesting.

Finally, the next logical step of the design would be to increase solar power capabilities with the addition of double hinged Solar Wings (as shown in Figure 6.1), which would represent a quantitative leap in performance and power-to-volume ratio, positioning the design as an even more attractive option and competing with actual cutting-edge PocketQube designs.

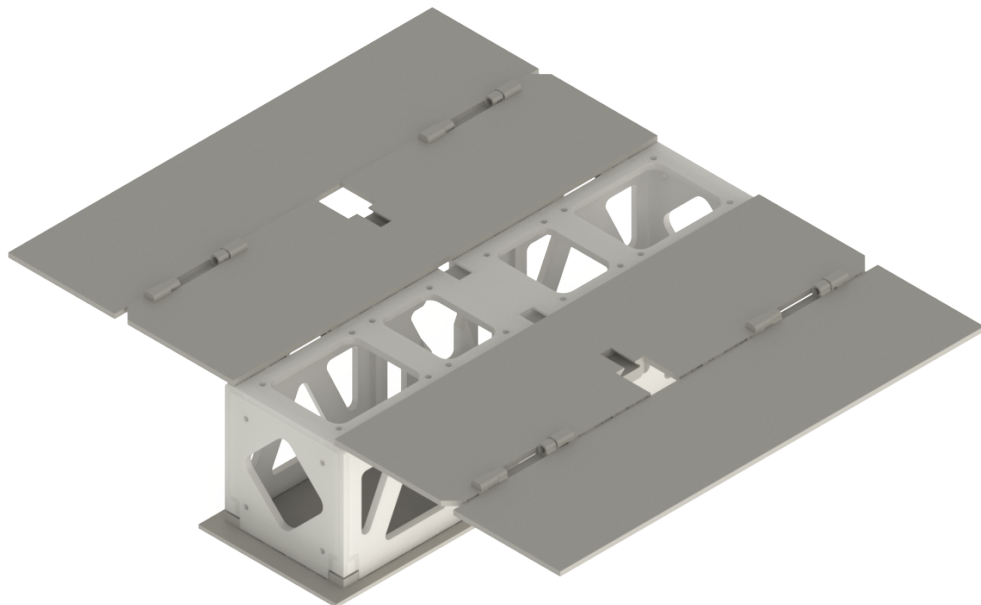


Figure 6.1: Preliminary concept of a 3P design with double-hinged solar wings (Source: Own elaboration)

Bibliography

1. KULU, Erik. *Nanosatellite & CubeSat Database* [online]. [N.d.]. [visited on 2024-03-20]. Available from: <https://www.nanosats.eu/database.html>.
2. CAPPELLETTI, Chantal; BATTISTINI, Simone; GRAZIANI, Filippo. Small launch platforms for micro-satellites. *Advances in Space Research*. 2018, vol. 62, no. 12, pp. 3298–3304. ISSN 0273-1177. Available from DOI: [10.1016/j.asr.2018.05.004](https://doi.org/10.1016/j.asr.2018.05.004).
3. SPERETTA, Stefano; SORIANO, Tatiana; BOUWMEESTER, Jasper; CARVAJAL-GODÍNEZ, Johan; MENICUCCI, Alessandra; WATTS, Trevor; SUNDARAMOORTHY, Prem; GUO, Jian; GILL, Eberhard. *CubeSats to PocketQubes: Opportunities and Challenges*. 2016.
4. *UniSat 5* [online]. [N.d.]. [visited on 2024-03-20]. Available from: https://space.skyrocket.de/doc_sdat/unisat-5.htm.
5. RADU, S; ULUDAG, M S; SPERETTA, S; BOUWMEESTER, J; MENICUCCI, A; CERVONE, A; DUNN, A; WALKINSHAW, T. PocketQube Standard. 2018.
6. *TU Delft*. [N.d.]. Available also from: <https://www.tudelft.nl/en/>.
7. *Alba Orbital* [online]. [N.d.]. [visited on 2024-03-20]. Available from: <http://www.albaorbital.com>.
8. *GAUSS Srl*. [N.d.]. Available also from: <https://www.gausssteam.com/>.
9. BOUWMEESTER, J.; RADU, S.; ULUDAĞ, Mehmet; CHRONAS, N.; SPERETTA, Stefano; MENICUCCI, Alessandra; GILL, Eberhard. Utility and constraints of PocketQubes. *CEAS Space Journal*. 2020, vol. 12. Available from DOI: [10.1007/s12567-020-00300-0](https://doi.org/10.1007/s12567-020-00300-0).
10. *PocketQube (PocketQub) - Gunter's Space Page* [online]. [N.d.]. [visited on 2024-03-20]. Available from: https://space.skyrocket.de/doc_sat/pocketqub.htm.
11. *Soluciones de IoT Satelital — FOSSA Systems* [online]. [N.d.]. [visited on 2024-03-20]. Available from: <https://fossa.systems/es/>.
12. *Stara: Space infrastructure as a service* [online]. [N.d.]. [visited on 2024-03-20]. Available from: <https://www.stara.space/>.
13. *Innova Space* [online]. [N.d.]. [visited on 2024-03-20]. Available from: <https://www.innova-space.com/es/>.
14. *Home Page - Hello Space* [online]. 2023. [visited on 2024-03-20]. Available from: <https://hellospace.ist/>.
15. KOHLA, Frederik; KUIJER, Thom; RAVEN, Tramper. *Design Document - Deployable Solarwings*. 2023.

16. ROIBAS, Elena; ALVAREZ, Jose Miguel; MARÍN COCA, Sergio; PORRAS-HERMOSO, Angel; PÉREZ-ÁLVAREZ, Javier; CUBAS, Javier; PINDADO, Santiago. The UPMQube: An Academic/Educational PocketQube Proposal for the EU2Space Challenge. *Athens Journal of echnology & Engineering*. 2023, vol. 10, pp. 27–48. Available from DOI: 10.30958/ajte.10-1-2.
17. MATEO VAZQUEZ, Sergio. *Assembly, Integration, Verification, and Testing of a 1P PocketQube* [online]. 2023. [visited on 2024-03-12]. Available from: <https://upcommons.upc.edu/handle/2117/400627>. Bachelor thesis. Universitat Politècnica de Catalunya. Accepted: 2024-01-31T12:13:34Z.
18. AGUIRRE GARNICA, Santiago; FREEMAN, Josh; REILLY, Colin; SCHWEGMAN, Maxwell; SHI, Benjamin. Horus: An Origami-Unfolding Solar Array For Autonomous Deployment on Mars. 2018. Available also from: <https://dataspace.princeton.edu/handle/88435/dsp01dj52w744g>. Accepted: 2018-08-20T14:11:08Z.
19. *Redwire's Innovative Solar Array Technology Powering the Future of Space Exploration*. 2022. Available also from: <https://redwirespace.com/newsroom/redwires-innovative-solar-array-technology-powering-the-future-of-space-exploration/>.
20. *Yim Space*. [N.d.]. Available also from: <https://www.shyimspace.com/FLEXIBLE-GaAs-SOLAR-CELL-pd574442698.html>.
21. *IKAROS Mission Overview*. [N.d.]. Available also from: https://www.jaxa.jp/countdown/f17/overview/ikaros_e.html.
22. *Azurspace Space Solar Cells*. [N.d.]. Available also from: <https://www.azurspace.com/index.php/en/products/products-space/space-solar-cells>.
23. *Spectrolab Photovoltaics*. [N.d.]. Available also from: <https://www.spectrolab.com/photovoltaics.html>.
24. *Space Mission Analysis and Design, 3rd edition*. 3rd edition. El Segundo, Calif.: Dordrecht; Boston: Microcosm, 1999. ISBN 978-1-881883-10-4.
25. *Fundamentals of Space Systems*. New York: Oxford University Press, 1994. ISBN 978-0-19-507497-0.
26. JEONG, Ju Won; YOO, Young Ik; LEE, Jung Ju; LIM, Jae Hyuk; KIM, Kyung Won. Development of a Tape Spring Hinge with a SMA Latch for a Satellite Solar Array Deployment Using the Independence Axiom. *IERI Procedia*. 2012, vol. 1, pp. 225–231. ISSN 2212-6678. Available from DOI: 10.1016/j.ieri.2012.06.035.
27. JEONG, Ju Won; YOO, Young Ik; SHIN, Dong Kil; LIM, Jae Hyuk; KIM, Kyung Won; LEE, Jung Ju. A novel tape spring hinge mechanism for quasi-static deployment of a satellite deployable using shape memory alloy. *The Review of Scientific Instruments*. 2014, vol. 85, no. 2, p. 025001. ISSN 1089-7623. Available from DOI: 10.1063/1.4862470.
28. BEMENT, L. J.; NEUBERT, V. H. Development of low-shock pyrotechnic separation nuts. In: 1973. Available also from: <https://ntrs.nasa.gov/citations/19740003570>. NTRS Author Affiliations: NASA Langley Research Center, Pennsylvania State Univ. NTRS Document ID: 19740003570 NTRS Research Center: Legacy CDMS (CDMS).

29. FOUCHÉ, F; HAUTCOEUR, A; CHASSOULIER, D; BLANC, A; SICRE, J. DEVELOPMENT AND TESTING OF A HIGH-TEMPERATURE SHAPE MEMORY ACTUATOR USING CN-250X FOR HOLD DOWN AND RELEASE MECHANISMS (HRM). [N.d.].
30. THURN, Adam; HUYNH, Steve; KOSS, Steve; OPPENHEIMER, Paul; BUTCHER, Sam; SCHLATER, Jordan; HAGAN, Peter. A Nichrome Burn Wire Release Mechanism for CubeSats. [N.d.].
31. CHANG, Bob; LAUGHLIN, Patrick; SASAKI, Terry. LOW SHOCK NON-EXPLOSIVE ACTUATOR. [N.d.].
32. KIM, Dongjin; JEONG, Donghee; LEE, Yeungjo; LEE, Youngwoo. Study on the Performance Evaluation of the Explosive Bolt that has been Natural Aging. *Journal of the Korean Society of Propulsion Engineers*. 2017, vol. 21, pp. 84–90. Available from DOI: 10.6108/KSPE.2017.21.3.084.
33. BHATTARAI, Shankar; KIM, Hongrae; JUNG, Sung-Hoon; OH, Hyun-Ung. Development of Pogo Pin-Based Holding and Release Mechanism for Deployable Solar Panel of CubeSat. *International Journal of Aerospace Engineering*. 2019, vol. 2019, e2580865. ISSN 1687-5966. Available from DOI: 10.1155/2019/2580865.
34. *Bambu X1 Carbon*. [N.d.]. Available also from: <https://eu.store.bambulab.com/en-es/products/x1-carbon-combo>.
35. *TU Delft - Delfi-PQ*. [N.d.]. Available also from: <https://www.tudelft.nl/lr/delfi-space/delfi-pq>.
36. *FandWay 410 Piezas Tornillos de Cabeza Hexagonal M2 Tornillo Allen Cilíndrico con Hexágono Interio de Acero Inoxidable 304, Tornillos de Máquina, Tuercas y Arandelas con 1 llaves Allen*. [N.d.]. Available also from: https://www.amazon.es/dp/B09SH63QSK?psc=1&ref=ppx_yo2ov_dt_b_product_details.
37. *ruthex M2 Gewindeeinsatz – 70 Stück RX-M2x4 Messing Gewindeguss für 3D Druck-Teile aus Kunststoff*. [N.d.]. Available also from: <https://www.ruthex.de/products/ruthex-gewindeeinsatz-m2-70-stuck-rx-m2x4-messing-gewindeguss>.
38. *Bobina de cuerda de nylon 0,35 mm x 100 m*. [N.d.]. Available also from: <https://www.apli.com/es/producto/13808>.
39. *YOKIVE 100uds Carbono Película Resistores, 1/4W 100 Ohm*. [N.d.]. Available also from: https://www.amazon.es/dp/B0BMXDTM9T?psc=1&ref=ppx_yo2ov_dt_b_product_details#Ask.
40. *ANSYS*. [N.d.]. Available also from: <https://www.ansys.com/>.
41. *Falcon User's Guide* [<https://www.spacex.com/media/falcon-users-guide-2021-09.pdf>]. 2021. [Accessed 21-05-2024].
42. ARGELICH ABAD, Pol. *Study of commercially available FDM 3D printing polymers for their use on small satellites for the HORUS Project*. 2024. Available also from: <https://upcommons.upc.edu/handle/2117/403994>. Bachelor thesis. Universitat Politècnica de Catalunya. Accepted: 2024-03-08T11:23:41Z.
43. Test Requirements for Launch, Upper-Stage, and Space Vehicles. [N.d.].
44. *Mission Success Handbook for Cubesat Missions*. [N.d.]. Available also from: <https://standards.nasa.gov/standard/GSFC/GSFC-HDBK-8007>.

45. *What is Random Vibration Testing?* [N.d.]. Available also from: <https://vibrationresearch.com/resources/what-is-random-vibration-testing/>.
46. *Brüel and Kjær - Modal Exciter 4825.* [N.d.]. Available also from: <https://www.bksv.com/en/instruments/vibration-testing-equipment/modal-exciters/modal-exciter-4825-4826>.
47. *Small Satellites, Big Impact: Sustainability in the Space Economy.* 2023. Available also from: <https://newspaceeconomy.ca/2023/04/14/small-satellites-big-impact-sustainability-in-the-space-industry/>.
48. *The space economy is booming. What benefits can it bring to Earth?* 2022. Available also from: <https://www.weforum.org/agenda/2022/10/space-economy-industry-benefits/>.
49. *Sustainability in Space.* [N.d.]. Available also from: <https://www.bsr.org/en/emerging-issues/sustainability-in-space-the-next-frontier>.
50. *New Space Debris Mitigation Policy and Requirements in effect.* [N.d.]. Available also from: <https://esoc.esa.int/new-space-debris-mitigation-policy-and-requirements-effect>.
51. *Collision risk from space debris: Current status, challenges and response strategies.* Lausanne: International Risk Governance Center (IRGC), 2021. Available from DOI: 10.5075/epfl-irgc-285976.
52. POLAT, Halis; VIRGILI-LLOP, Josep; ROMANO, Marcello. Survey, Statistical Analysis and Classification of Launched CubeSat Missions with Emphasis on the Attitude Control Method. *Journal of Small Satellites*. 2016, vol. 5, pp. 513–530.
53. BEDI, Rajan. *Using commercial-off-the-shelf components for space: a technical look.* 2018. Available also from: <https://www.spacetechasia.com/using-commercial-off-the-shelf-components-for-space-applications/>.